

## RESEARCH ARTICLE

10.1002/2017JB014959

## Key Points:

- Multichannel seismic imaging reveals the seismostratigraphy architecture of La Réunion volcanoclastic apron
- Prevalence of gradual degradation/dismantling processes on large flank collapse events
- Control of La Réunion present-day morphology by a major proto Piton des Neiges-Piton des Neiges volcanic complex

## Supporting Information:

- Supporting Information S1

## Correspondence to:

E. Lebas,  
elodie.lebas@ifg.uni-kiel.de

## Citation:

Lebas, E., Le Friant, A., Deplus, C., & de Voogd, B. (2018). Understanding the evolution of an oceanic intraplate volcano from seismic reflection data: A new model for La Réunion, Indian Ocean. *Journal of Geophysical Research: Solid Earth*, 123, 1035–1059. <https://doi.org/10.1002/2017JB014959>


Received 6 SEP 2017

Accepted 18 JAN 2018

Accepted article online 24 JAN 2018

Published online 20 FEB 2018

## Understanding the Evolution of an Oceanic Intraplate Volcano From Seismic Reflection Data: A New Model for La Réunion, Indian Ocean

E. Lebas<sup>1,2</sup> , A. Le Friant<sup>1</sup>, C. Deplus<sup>1</sup>, and B. de Voogd<sup>3</sup>

<sup>1</sup>Institut de Physique du Globe de Paris, Sorbonne Paris Cité and CNRS UMR 7154, Paris, France, <sup>2</sup>Now at Institut für Geowissenschaften, Christian-Albrechts-Universität zu Kiel, Kiel, Germany, <sup>3</sup>Université de Pau et des Pays de l'Adour, CNRS FR 2952, Pau, France

**Abstract** High-resolution seismic reflection profiles gathered in 2006 on La Réunion submarine flanks and surrounding abyssal plain, enabled characterization of the seismostratigraphy architecture of the volcanoclastic apron. Four seismic units are defined beyond the edifice base: (1) a basal unit, interpreted as pelagic sediment predating La Réunion volcanism; (2) a second unit showing low- to medium-amplitude reflections, related to La Réunion emergence including the submarine explosive phase; (3) a high-amplitude seismic unit, associated with subaerial volcanic activity (i.e., mature island stage); and (4) an acoustically transparent unit, ascribed to erosion that currently affects the volcanic complex. Two prominent horizons delineate the base of the units II and III marking, respectively, the onset of La Réunion seamount explosive activity and the Piton des Neiges volcanic activity. Related isopach maps demonstrate: (1) the existence of a large proto-Piton des Neiges volcano during the first building phase of the volcanic complex, and (2) the central role of the Piton des Neiges volcano during the second phase. Shield growth stage of the Piton de la Fournaise volcano is also captured in the upper part of the volcanoclastic apron, attesting to its recent contribution. Seismic facies identified in the apron highlight a prevalence of sedimentary and reworking processes since the onset of the volcanism compared to catastrophic flank collapses. We present here a new model of evolution for La Réunion volcanic complex since the onset of the volcanism and argue that a major proto Piton des Neiges-Piton des Neiges volcanic complex controls La Réunion present-day morphology.

### 1. Introduction

The first models of evolution proposed for volcanic islands were based on geological and geomorphological studies (e.g., Rivals, 1950; Stearns, 1946; Upton & Wadsworth, 1965). Later complemented by geochronological data, they provided spatial and temporal constraints on the subaerial volcanic activity (Germa et al., 2011). Data gathered by oceanographic cruises during the last decades showed that subaerial parts of volcanic islands represent a small percentage of the total edifice volume compared to the submarine parts (3% for La Réunion, de Voogd et al., 1999; ~2% for Gran Canaria, Krastel & Schmincke, 2002; ~15% for Vulcano, Romagnoli et al., 2013). Investigations of submarine flanks are therefore required to assess the whole history of volcanic islands and to propose a complete model of their evolution. For instance, hummocky topographies on swath bathymetry and hyperbolic facies on subbottom profiles are characteristic of mass-wasting deposits (Deplus et al., 2001; Masson et al., 2002; Moore et al., 1989, 1994). Such deposits can cover hundreds of square kilometers, reach volumes of thousands of cubic kilometers, and are common and recurrent during the whole evolution of volcanic islands (McGuire, 1996). Understanding the evolution of volcanic islands therefore requires the combined analysis of marine geophysical data sets with terrestrial observations.

However, fundamental questions remain unanswered as regards the location of the main volcanic activity during the early phases of an island growth: Where was the main volcanic center located at the initiation of the volcanism? Was only one volcanic center present? If not, how many were they? How did they evolve through time? Did they experience large flank collapses? What was the respective role of gradual erosion/dismantling processes versus catastrophic collapses during the different building phases?

Submarine aprons surrounding oceanic islands are directly derived from volcanic activity and dismantling processes of both the subaerial and submarine parts (Menard, 1956). They reflect the long-term evolution of volcanic islands and therefore are keys to tackle the above questions. Nature and internal architecture of apron units can be assessed through drilling and acquisition of seismic data (e.g., Funck et al., 1996;

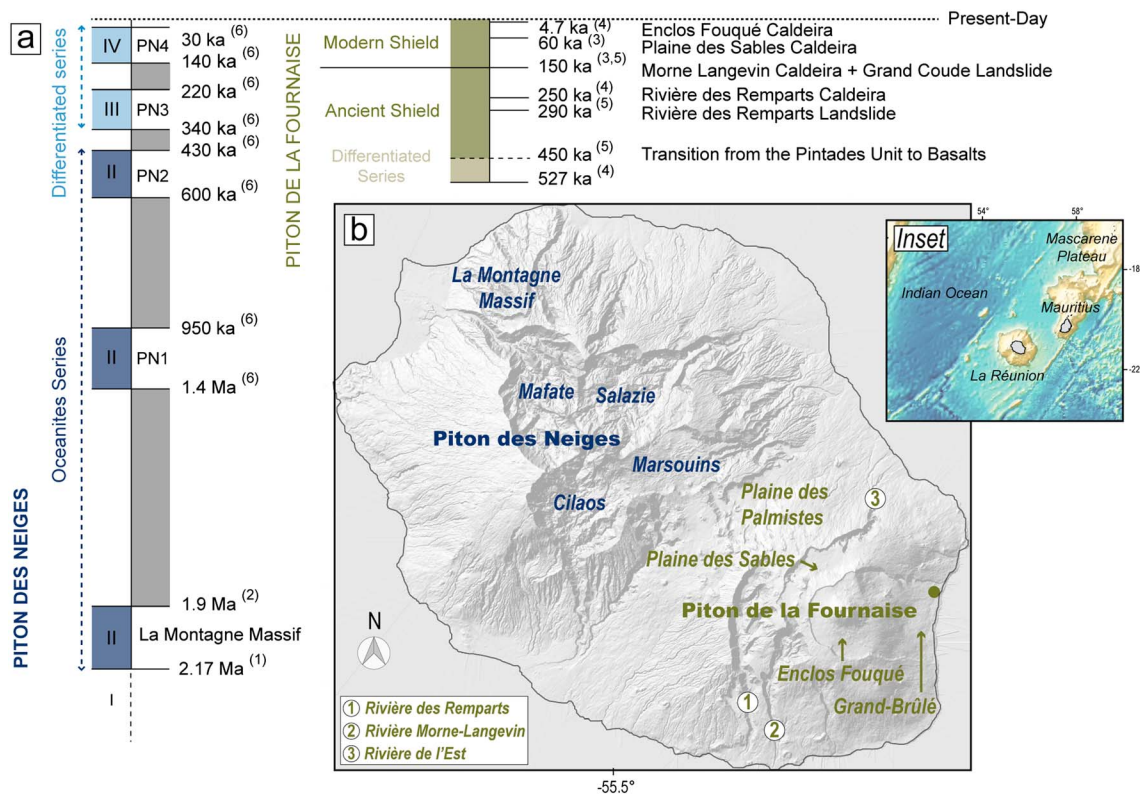


**Figure 1.** (a) Building phases (color) and erosional intervals (gray) related to the Piton des Neiges (blue) and the Piton de la Fournaise (green) volcanoes from on-land observations. Roman numerals correspond to the names of the building phases usually given in the literature for the Piton des Neiges. Light colors indicate differentiated series. Ages are from (1) Quidelleur et al. (2010), (2) McDougall (1971), (3) Bachèlery and Mairine (1990), (4) Gillot et al. (1994), (5) Merle et al. (2010), and (6) Salvany et al. (2012). (b) Main morphological structures identified on land are indicated in blue for the Piton des Neiges and in green for the Piton de la Fournaise. Green dot indicates the location of the Grand-Brûlé drill hole. Inset: Location of La Réunion Island in the Mascarene Basin (Indian Ocean) from predicted bathymetry (Smith & Sandwell, 1997).

Leslie et al., 2002; Rees et al., 1993; Schmincke & Sumita, 1998; Urgeles et al., 1998; Wolfe et al., 1994). For instance, correlations between seismic data, drilled lithologies, and onshore observations identify specific periods in the Canary Islands volcanism within the apron providing insights on their evolution (Funck et al., 1996; Urgeles et al., 1998).

This contribution aims to provide new insights on the evolution of an isolated oceanic intraplate volcano from investigations of its volcanoclastic apron, based on results from La Réunion. Analysis of the seismic data gathered during the FOREVER cruise allows us to study the processes captured in the offshore sediment record and to propose a new model of evolution of La Réunion volcanic complex since the onset of the volcanism.

## 2. Previous Models of Evolution

La Réunion Island is located in the Mascarene Basin, in the Indian Ocean, approximately 750 km east from Madagascar (Figure 1, inset). It is thought to have formed from a mantle plume that was also responsible for the Deccan Traps (~65 Ma), the Laccadives, Maldives (~55–60 Ma) and Chagos (~47–48 Ma) Ridges, the Mascarene Plateau (~35 Ma), and the Mauritius Island (~7–8 Ma) (Duncan et al., 1989).

The first models of evolution proposed for La Réunion were based on geomorphological (Rivals, 1950) and geological studies (Upton & Wadsworth, 1965, 1969) and identified two main volcanoes on the island: the Piton des Neiges and the active Piton de la Fournaise (Figure 1b). Results from successive geochronological studies complemented these models, providing temporal and spatial constraints on the evolution of the two volcanoes (Figure 1a) (Gillot et al., 1994; Gillot & Nativel, 1989; McDougall, 1971; Salvany et al., 2012). The oldest subaerial lava flows were dated at  $2.17 \pm 0.03$  Ma (Quidelleur et al., 2010) and found in La Montagne Massif (Figure 1b). This massif represents ~5% of the present-day island surface area and was interpreted as the remnant of a proto-Piton des Neiges volcano, referred to as La Montagne (2.1–1.9 Ma; Gillot

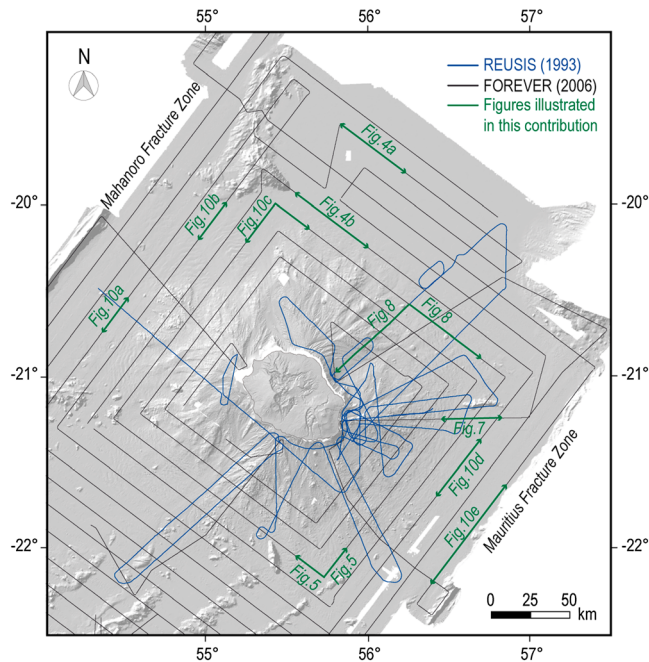


**Figure 2.** Location of the seismic profiles collected during the REUSIS (1993) and FOREVER (2006) cruises. Green lines correspond to the location of the seismic profiles illustrated in this contribution.

et al., 1994). According to Gillot et al. (1994) and Salvany et al. (2012), La Montagne edifice experienced, at least, one catastrophic flank collapse at 1.8 Ma. Following a period of quiescence in volcanic activity of  $\sim 500$  ka, the Piton des Neiges was emplaced between 1.4 Ma and 30 ka (Salvany et al., 2012), and is now located in the northwestern part of the island. Its volcanic activity is divided in two main stages (Figure 1a). The first stage (1.4–0.43 Ma; based on the interpretation of La Montagne volcano as being the subaerial protoedifice of Piton des Neiges) corresponds to the shield building phase, and mainly consisting of emissions of aphyric and olivine-rich basaltic lava flows, known as the *Oceanites Series* (McDougall, 1971). Salvany et al. (2012) distinguished two building phases (PN1: 1.4–0.95 Ma and PN2: 600–430 ka) during that period (Figure 1a). A period of quiescence and intense erosion of  $\sim 90$  ka separates the two stages. From 430 ka to 30 ka the Piton des Neiges stratovolcano was emplaced. Two building phases (PN3: 340–220 ka and PN4: 140–30 ka) have also been distinguished (Salvany et al., 2012) during this second period (Figure 1a). Lavas from basalts to trachytes were emitted during this period, also known as the *Differentiated Series*.

The Piton de la Fournaise volcano was built contemporaneously to the volcanic activity of Piton des Neiges (Figure 1a). Radiogenic ages obtained on F-rich lava flows recognized within the Rivière des Remparts, Rivière de l'Est, and Rivière Morne-Langevin (Figure 1b) dated the onset of the Piton de la Fournaise volcanic activity at, at least, 527 ka (Gillot & Nativel, 1989). Merle et al. (2010) recently proposed a younger age of 450 ka. The volcanic activity of Piton de la Fournaise is also divided in two main stages (Bachèlery & Mairine, 1990; Gillot & Nativel, 1989; Gillot et al., 1994; Figure 1a). The first stage (527 ka–150 ka) corresponds to the building of the Ancient Shield volcano, whose volcanic center was located near the present-day site of the Plaine des Sables (Bachèlery & Mairine, 1990; Figure 1b). During the second stage (150 ka to present), the Modern Shield edifice was emplaced leading to the current Piton de la Fournaise. A migration of the volcanic activity toward the east was identified between the two stages. Four volcanotectonic structures opened to the east were observed on its eastern flank. From west to east, they correspond to the Morne-Langevin, Rivière des Remparts, Plaine des Sables, and Enclos-Fouqué/Grand-Brûlé structures (Figure 1b).

The geothermal exploration carried out in the Grand-Brûlé area, in the eastern part of Piton de la Fournaise (Figure 1b), included investigation of the flank lithostratigraphy from drill hole data. Drilled lithologies revealed the presence of a layered intrusive complex mainly composed of gabbro cumulates from 1,010 m down to 3,003.5 m (Rançon et al., 1989). This complex was interpreted as a former, shallower magma chamber of an ancient edifice referred to as proto-Fournaise by Rançon et al. (1989); a large positive gravimetric anomaly identified by Rousset et al. (1987) supported the interpretation. Geophysical data gathered subsequently complemented the previous findings. From interpretations of gravimetric and magnetic data, Malengreau et al. (1999), Lénat et al. (2001), and Gailler and Lénat (2010, 2012) associated this intrusive complex to an older volcanic edifice, referring to it as Les Alizés. Lénat et al. (2001) proposed an age older than 0.78 Ma for Les Alizés volcano from magnetic observations and a size similar to the present-day Piton des Neiges, based on similitudes observed between the dimensions of the two gravimetric anomalies recognized. The lack of on-land evidence of Les Alizés volcano led Lénat et al. (2001) to propose a complete dismantlement of the volcanic edifice by, at least, one large flank collapse. In their model, the Piton des Neiges, Les Alizés and Piton de la Fournaise volcanoes were all affected by large, subaerial flank collapses whose related deposits accumulated offshore, leading to the formation of the four submarine bulges identified by Labazuy (1996) on the bathymetry.

Over the last decades, several research cruises carried out offshore La Réunion investigated the submarine terrains. Debris avalanche deposits were identified offshore Piton de la Fournaise during the Fournaise 1 and Fournaise 2 cruises (Labazuy, 1996; Lénat et al., 1989). Seismic data collected during the REUSIS cruise

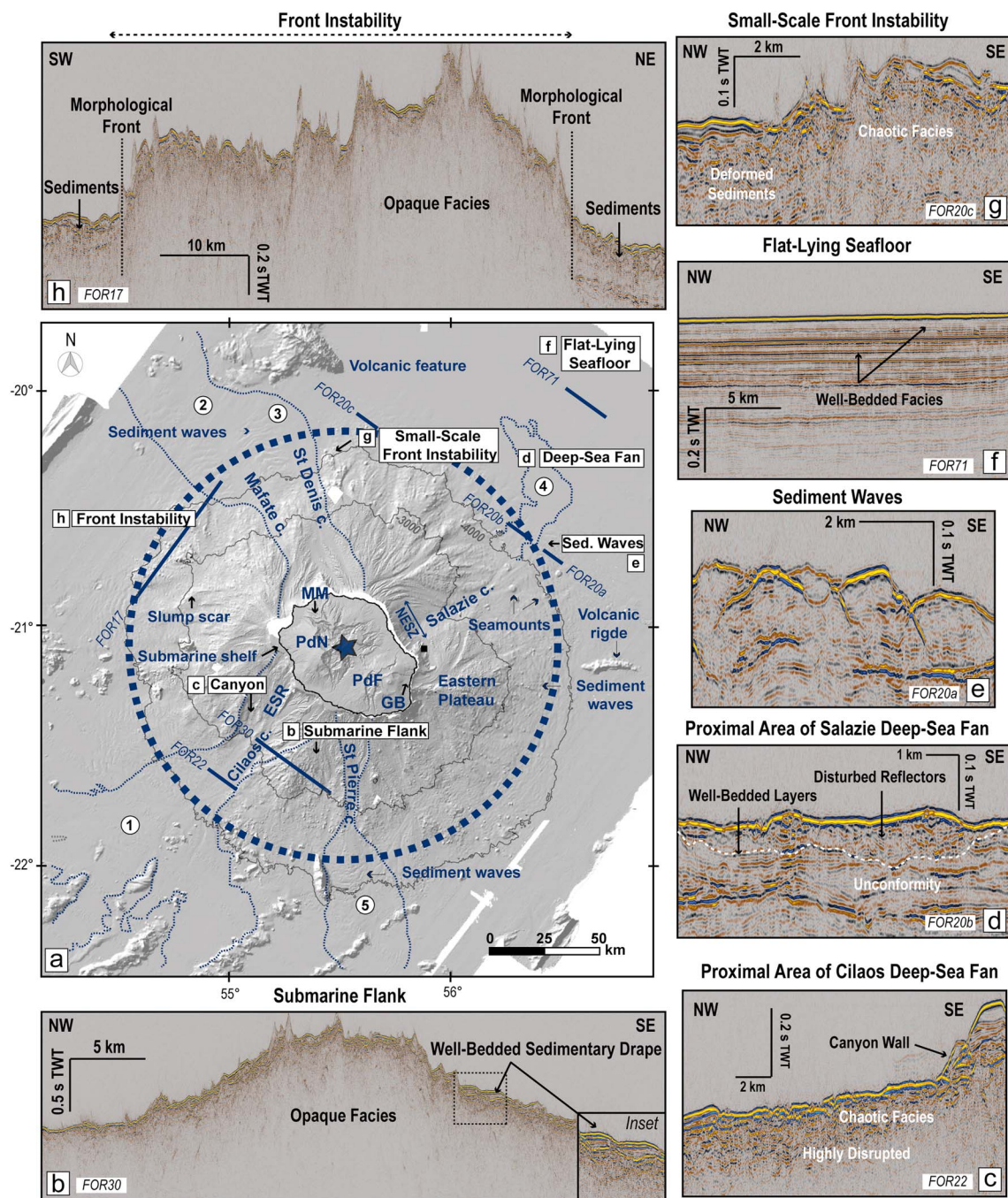


**Figure 3.** (a) Combined bathymetry (FOREVER and ERODER1 cruises) and topography data of La Réunion volcanic complex illuminated from NW. Dashed thick circle indicates the base of the volcanic complex as delimited by Le Friant et al. (2011). Note the coincidence between the center of the circle, shown by the blue star, and the summit area of the Piton des Neiges. Black square indicates the location of the oldest submarine dredged sample dated at 3.77 Ma by Smetana (2011). Thin dashed lines delimit the turbidite systems identified by Sisavath et al. (2011) and Mazuel et al. (2016). The numbers 1–5 correspond, respectively, to the deep-sea fans of Cilaos, Mafate, Saint-Denis, Salazie, and Saint-Joseph. ESR: Etang Salé Ridge. MM: La Montagne Massif. PdN: Piton des Neiges. PdF: Piton de la Fournaise. GB: Grand-Brûlé. NESZ: NE Sedimentary Zone. Cilaos c.: Cilaos canyon; same for Mafate c., St Denis c., Salazie c., and St Pierre c. (c.: canyon). (b–h) Seismic profiles illustrating the seismic expression of the main morphological features of the seafloor discussed in the text.

captured the sediment record offshore La Réunion down to the oceanic basement, in the eastern region and a part of the southern one (de Voogd et al., 1999; Figure 2). A prominent horizon, named V, was recognized and interpreted as the top of sedimentary units predating the volcanism (de Voogd et al., 1999). The lack of angular unconformities within the apron revealed the absence of flexure of the lithosphere under the load of

La Réunion volcanic edifice (de Voogd et al., 1999) contrary to previous suggestions (e.g., Bonneville et al., 1988). Velocity models derived from the REUSIS OBS and on-land data supported this interpretation (Charvis et al., 1999; Gallart et al., 1999).

From a compilation of all the marine geophysical data sets available prior to 2006, Oehler et al. (2008) proposed that at least 47 mass-wasting events affected La Réunion, 37 of which had a submarine origin. Giant landslides were therefore considered a major and recurrent process during the whole evolution of the volcanic edifice. However, the data available prior to 2006 solely covered the southeastern flank and a section to the southwest; the northeastern and northwestern flanks being only constrained by few isolated profiles (e.g., Figure 1 in Oehler et al., 2008).

The FOREVER cruise was thus carried out in 2006 and provided for the first time full coverage of La Réunion submarine flanks and surrounding abyssal plain (Figure 2). Five large deep-sea fans (numbered 1 to 5 in Figure 3a) were discovered offshore La Réunion from combined analysis of swath bathymetry, backscatter, and 3.5 kHz echo sounder data (Mazuel et al., 2016; Saint-Ange et al., 2011; Sisavath et al., 2011). Sea bottom morphology analysis performed by Le Friant et al. (2011) showed that the base of the volcanic edifice (defined as the slope transition between the volcanic complex and the surrounding seafloor) could be approximated by a circle with a radius of  $\sim 100$  km (dashed circle in Figure 3a). Contrary to its elongated sub-aerial form, La Réunion submarine base has a circular shape. The center of the circle is located at the summit area of Piton des Neiges, suggesting that the Piton des Neiges was the main volcano on which evolved the entire complex of La Réunion. Chaotic deposits, recognized offshore the active Piton de la Fournaise volcano (e.g., Labazuy, 1996; Lénat et al., 1989; Oehler et al., 2004, 2008) extend far away beyond the edifice base while elsewhere, chaotic deposits do not extend on the abyssal plain as pointed out by Le Friant et al. (2011). The absence of chaotic deposits on the abyssal plain offshore Piton des Neiges led these authors to propose two distinct behaviors for the volcanoes: while Piton de la Fournaise experienced catastrophic flank collapses, the Piton des Neiges would be affected by slow deformation processes such as sliding and spreading.

The geomorphological and geochronological study performed by Salvany et al. (2012) underlined the absence of large subaerial flank collapses from the Piton des Neiges since 1.4 Ma, possibly longer. The authors considered erosion and particularly gradual disintegration as a prevailing factor during the whole evolution of the Piton des Neiges, having greatly contributed to shape its present-day morphology.

### 3. Data Acquisition and Processing

The FOREVER cruise onboard French R/V L'Atalante (2006) collected a dense network of marine geophysical data (swath bathymetry, backscatter, 3.5 kHz echo sounder, seismic, gravity, and magnetic data) on La Réunion submarine flanks and surrounding abyssal plain (Deplus, 2006). The 24-channel, high-resolution seismic reflection profiles, with a total length of 12,200 km, were gathered using three different configurations (Figure 2 and Table 1). Most profiles (1–54 and 61–64) were acquired using two GI air gun sources (45/45 and 105/105 in.<sup>3</sup>) towed at  $\sim 6$  m below the sea surface, with a shot spacing of 10 s ( $\sim 50$  m). A few profiles (55–60 and 65–73) were acquired with slightly different source configurations, as detailed in Table 1. All data were filtered, stacked, and migrated using seawater velocity (1,500 m/s) within the Seismic Unix software<sup>©</sup> (Cohen & Stockwell, 1996). Navigation was based on GPS data providing a positioning accuracy of a few meters.

The 96-channel, seismic reflection profiles, with a total length of 2,500 km, were previously collected on the southeastern and southwestern submarine flanks, up to  $\sim 50$  km from the edifice base during the REUSIS cruise (R/V Marion Dufresne, 1993; Figure 2). Source and recording parameters are summarized in Table 1 and details on data processing may be found in de Voogd et al. (1999).

### 4. Architecture of La Réunion Volcaniclastic Apron

The high-resolution and full coverage of the FOREVER swath bathymetry and seismic data afford us a detailed characterization of La Réunion submarine flanks and surrounding seafloor morphology. Here we present the varying morphology of the seafloor and describe the related seismic expressions from the coastline toward the open sea.

**Table 1**  
Summary of the Acquisition Parameters of the Two Seismic Surveys Mentioned in This Contribution

Cruise	Set	Lines	Sources	Number of guns	Gun depth (m)	Streamer length (m)	Number of channels	Channel spacing (m)	Streamer depth (m)	Minimum offset (m)	Shot interval (s)	Average bandwidth of the processed data
REUSIS (1993)	1	W <sup>a</sup>	9 L (6) + 5 L (2)	8	10–20	2,400	96	25	25	270	20	10–30 Hz
	2	C/R <sup>a</sup>	16 L	8	10–20	2,400	96	25	25	270	80	10–30 Hz
FOREVER (2006)	1	1–54 + 61–64	45/45–105/105 (Cu,In) <sup>b</sup>	2	6	300	24	12,5	4–10	204–214	10	10–90 Hz
	2	55–56	35/35–105/105 (Cu,In) <sup>b</sup>	2	3	300	24	12,5	3–5	177	6	10–90 Hz
	3	57–60 + 65–73	105/105–45/45 (Cu,In) <sup>b</sup>	2	3	300	24	12,5	4–10	214–224	10	10–90 Hz

<sup>a</sup>de Voogd et al. (1999) and Pou Palomé (1997). <sup>b</sup>GI air gun volumes given as generator volume/injector volume.

#### 4.1. Seafloor Morphology and Related Seismic Expression Offshore La Réunion

A shallow submarine shelf extending to a water depth of ~100 m borders La Réunion Island (Oehler et al., 2008; Figure 3a). Offshore Piton des Neiges, the shelf is well developed with a maximum width of 7 km near La Montagne Massif (Figure 3a) and an average width of 2.5 km elsewhere (Oehler et al., 2008). Offshore Piton de la Fournaise, the shelf becomes narrower (0.5 km to 1 km) while it is entirely missing offshore the Grand-Brûlé. Oehler et al. (2008) ascribed its origin to repeated eustatic sea level fluctuations.

La Réunion submarine flanks show gentle slopes with an average of about 5° that extend down to a water depth of ~4,000 m. The dashed circle shown in Figure 3a indicates the base of the volcanic edifice (defined as the slope transition between the volcanic complex and the surrounding seafloor) as delimited by Le Friant et al. (2011). The volcanoclastic apron as described in the literature (e.g., Menard, 1956; Schmincke & Sumita, 1998) extends far beyond the slope transition. In the seismic data, a prominent and prevalent opaque facies overlain by thin chaotic reflections characterizes La Réunion submarine flanks (Figure 3b). This chaotic facies is draped in places by low- to medium-amplitude, wavy to subhorizontal, parallel seismic reflections (Figure 3b, inset).

Several canyons cut through the submarine flanks and delimit the upper parts of five large volcanoclastic turbidite systems named Cilaos, Mafate, Saint-Denis, Salazie, and Saint-Joseph (Figure 3a). These turbidite systems, also known as deep-sea fans, are clearly identifiable on the FOREVER backscatter sonar images (see Figure 1 in Saint-Ange et al., 2011 and Figure 2 in Sisavath et al., 2011). The Cilaos deep-sea fan corresponds to the largest turbidite system recognized offshore La Réunion. It covers an area of about 15,000 km<sup>2</sup> (Sisavath et al., 2011), three times more than the coalescent deep-sea fans of Mafate and Saint-Denis (Mazuel et al., 2016). A prevalent, acoustically opaque seismic facies overlain by chaotic reflections characterizes the head of the submarine canyons. In the proximal area of the turbidite systems, the seismic signature changes and a chaotic facies overlies highly disrupted reflections of variable amplitudes (Figure 3c). In the Salazie deep-sea fan, disturbed reflections truncate underlying layers (Figure 3d), attesting to the erosional character of the turbidites on the underlying units. This erosional unconformity disappears further north and only well-bedded reflections compose the distal part of the turbidite system. Bedded to well-bedded reflections also characterize the deep-sea fan of Cilaos. This seismic facies is comparable to the well-bedded facies encountered in the flat-lying part of the abyssal plain (Figure 3f).

Sediment waves observed around La Réunion are radially distributed (Figure 3a) and identified up to 30 km beyond the slope transition (Le Friant et al., 2011). Their dimensions are up to several kilometers in wavelength and tens of meters in amplitude. In the seismic data, low- to medium-amplitude, disrupted to subparallel, internal reflections characterize the sediment waves (Figure 3e). When located on the sides of sedimentary fan paths, such as

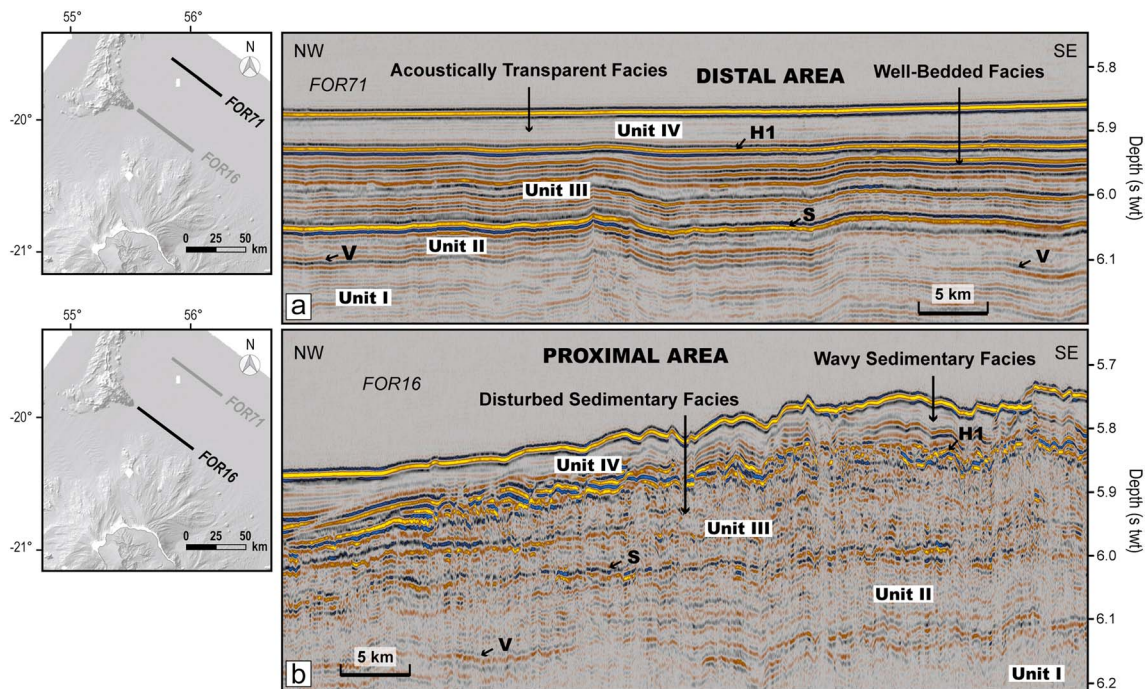


**Figure 4.** Seismic profiles showing the four seismostratigraphic units identified in the volcaniclastic apron offshore La Réunion Island (a) in the distal region and (b) in the proximal region. The basal unit I shows the lowest amplitudes, while the unit III shows the highest amplitudes. The last unit IV is characterized by a semitransparent facies, where internal reflections can be seen. The prominent horizons V and S bound the units II and III at a regional scale, while the horizon H<sub>1</sub> is only observed in the northern region. Note the reverse polarity of the horizon V in the northern distal region.

offshore the canyons of Mafate, Saint-Denis, and Saint-Pierre, the sediment waves can be related to active channel sedimentary processes (Mazuel et al., 2016; Saint-Ange et al., 2011). Elsewhere, Le Friant et al. (2011) ascribed their origin to unconfined turbidity flows on the flanks of the volcanic complex, which could be related to the spreading of the volcano that continuously dismantled the superficial part of the flanks. Chaotic terrains characterizing the submarine flanks would serve as irregularities to form these sediment waves.

Submarine landslides of variable sizes are widely observed around La Réunion and mainly recognized at the foot of the submarine flanks (Figure 3a). They correspond to the front instabilities described by Le Friant et al. (2011). A prevalent, acoustically opaque seismic facies characterizes the most voluminous landslides (Figure 3h), while the smaller instabilities show chaotic reflections of variable amplitudes (Figure 3g). Such signature is also observed at the toe of the large front instabilities, where the slumped mass desegregates to form hummocks (Figure 3a). Offshore the Piton de la Fournaise, the presence of hummocks is related to debris avalanche deposits resulting from flank collapses that affected the edifice (Labazuy, 1996; Le Friant et al., 2011; Lénat et al., 1989; Oehler et al., 2004, 2008).

#### 4.2. Seismic Sequence Analysis

Four units are recognized in the seismic data and numbered I to IV from the oldest to the youngest (Figure 4). The basal unit I displays relatively low-amplitude reflections. The second unit (II) shows low- to medium-amplitude reflections and is bounded at its base by a prominent horizon that we refer to as horizon V (Figures 4 and 5). Another strong reflection marks the upper boundary of the unit II and, consequently, the base of the unit III (Figure 4). We call this strong reflection horizon S. We delineate the horizons V and S all around the island (Figures 6a and 6b). In the eastern region, it is worth pointing out the striking undulated morphology of the horizon S (Figure 7). The third unit (III) identified shows higher-amplitude seismic reflections than the two previous units, which is particularly evident in the distal area, and is bounded at its top by another prominent reflection, which is clearly—but only—identified in the northern region (Figures 4 and 6c). We call this strong reflection, horizon H<sub>1</sub>, which scarcely displays an undulated morphology in the

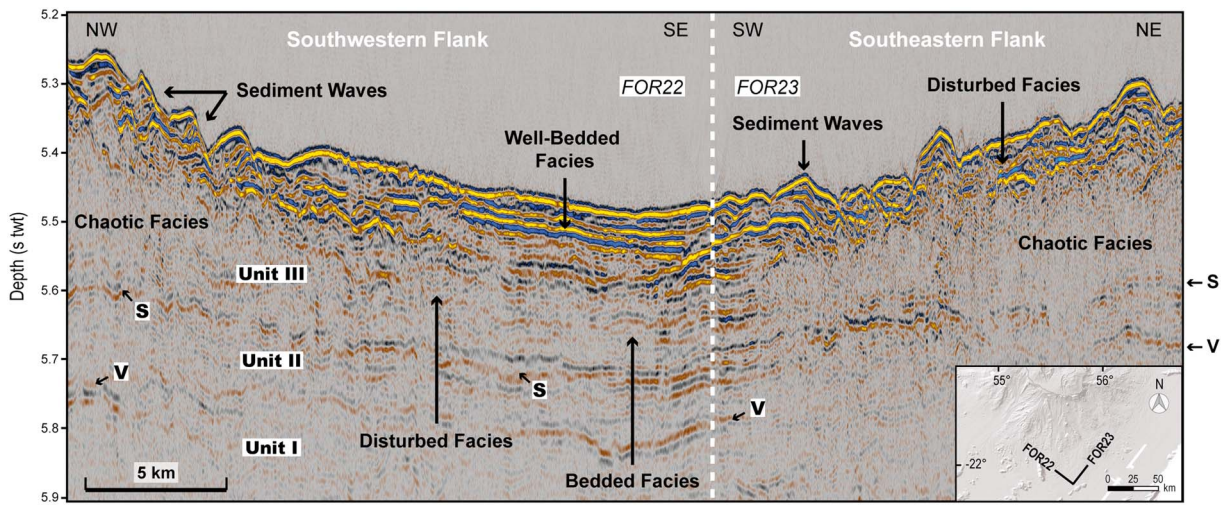


**Figure 5.** Continuity of the two prominent horizons V (deeper) and S (shallower) identified in the volcaniclastic apron between the southeastern and southwestern submarine flanks. Inset: Location of the seismic lines.

proximal area (Figure 4b). The youngest unit IV, which is not visible everywhere, exhibits an acoustically semitransparent facies, with low- to medium-amplitude, wavy to subhorizontal, parallel internal reflections (Figure 4). Two other horizons are identified locally in the southeastern region and correspond to the horizons H<sub>2</sub> and H<sub>3</sub> (Figures 6d, 6e, and 7).

Each horizon has been picked on the FOREVER seismic lines using the SMT Kingdom Suite software and correlated along strike and between parallel lines through comparisons of the seismic signatures of the units

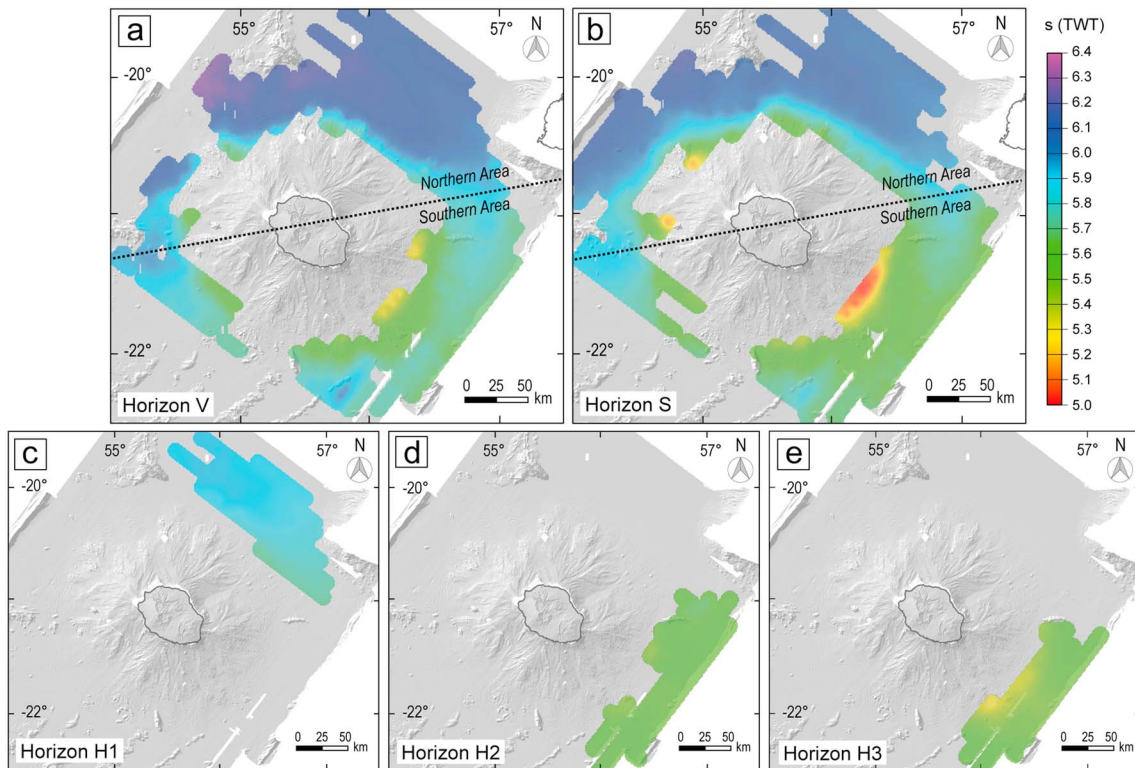


**Figure 6.** Extent and two-way travel time (TWT) for the horizons (a) V, (b) S, (c) H<sub>1</sub>, (d) H<sub>2</sub>, and (e) H<sub>3</sub> superimposed on shaded bathymetry. Dashed line separates the deeper northern region mentioned in the text from the shallower southern region. Because of the poor seismic imaging in the thickest parts of the edifice, the horizons have not been identified on the submarine flanks. Note the local character of the minor prominent horizons H<sub>1</sub>, H<sub>2</sub>, and H<sub>3</sub>, while the horizons V and S are regionally mapped.



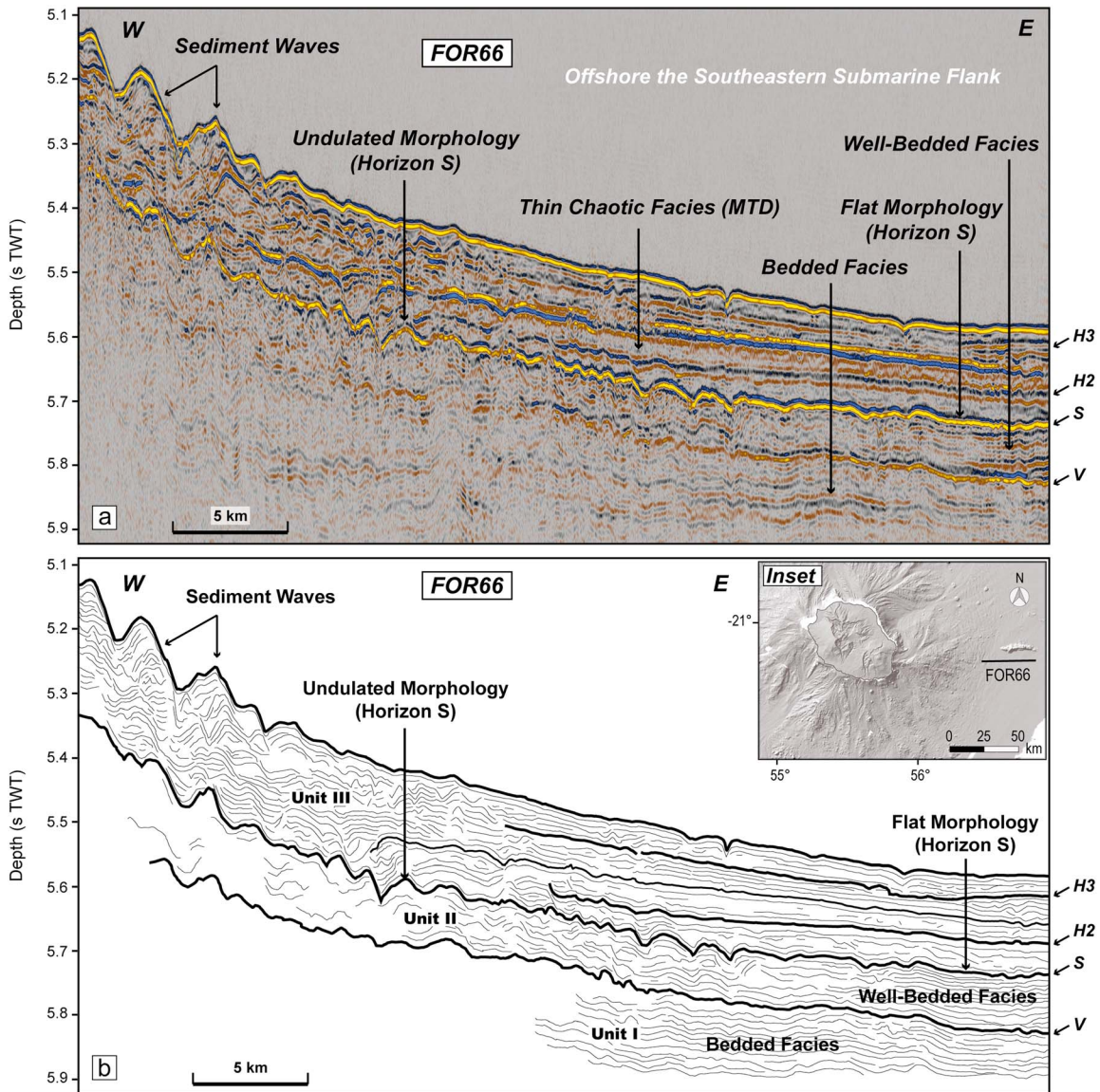


**Figure 7.** (a) Seismic profile FOR66 underlying the presence of local horizons H<sub>2</sub> and H<sub>3</sub> in the volcanoclastic apron east of La Réunion. While the horizons V and S are identified at a regional scale, the horizons H<sub>2</sub> and H<sub>3</sub> are only observed offshore the southeastern submarine flank. Note the high amplitude of the horizon S and its specific undulated morphology. High amplitudes are also noted for the horizon V. Note the absence of a superficial unit characterized by an acoustically semitransparent facies (like Unit IV in the northern region). (b) Interpretation of the seismic profile FOR66. Inset: Location of the seismic profile.

identified above and below. Two-way travel time (TWT) and geographic positioning for each horizon have been then extracted from the Kingdom Suite project. To corroborate the uniqueness of the horizons, a cross-over error analysis has been performed on the horizons TWT time using the radial seismic lines. TWT time differences at internal FOREVER crossover are less than 0.02 s and probably related to the picking. These low values attest to the recognition of the same horizons on the parallel seismic lines.

To investigate the depth variations of the horizons and the thickness of the seismostratigraphic units, we constructed regular grids using the GMT software (Wessel & Smith, 2004) with a grid spacing of 10 km, which results from the mean distance between adjacent seismic lines.

#### 4.3. Tie With the REUSIS Data

Parts of the eastern and southern regions of the volcanoclastic apron were previously imaged down to the oceanic crust during the REUSIS cruise, but at a lower resolution (e.g., de Voogd et al., 1999). Difference in

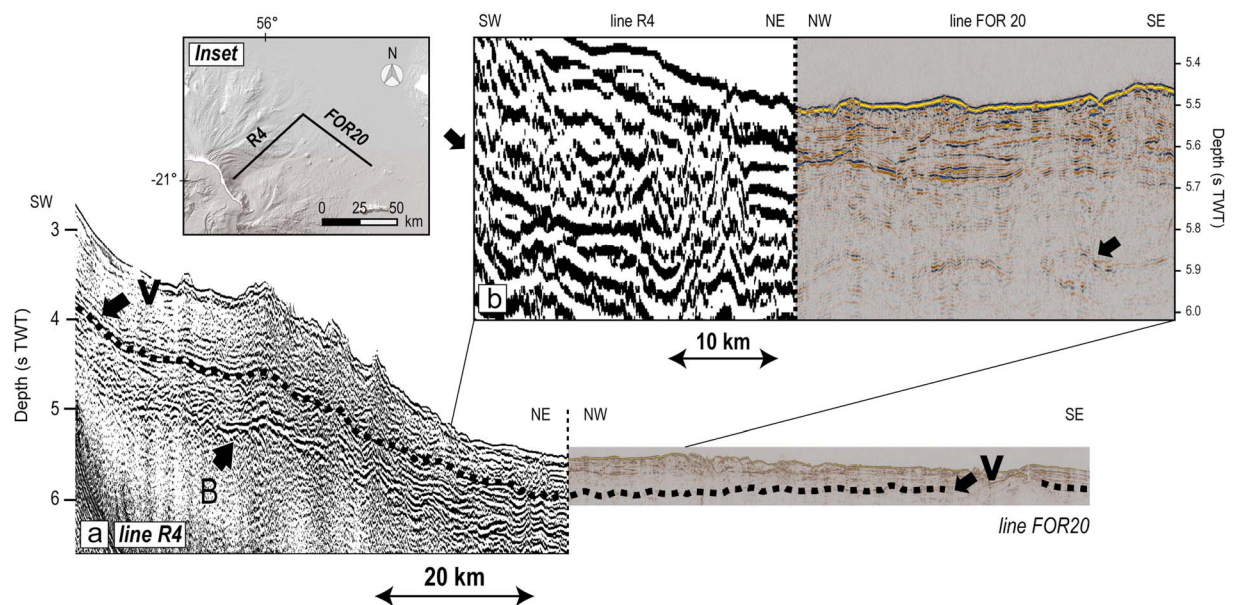


**Figure 8.** (a) Correlation of the deeper horizon V identified on the FOREVER seismic lines to the horizon also named V in the REUSIS profile R4 (modified from Pou Palomé, 1997). Black arrow labeled B indicates the top of the oceanic basement from de Voogd et al. (1999), while other black arrows represent the horizon V identified in our data and in the REUSIS profile. Poor signal penetration in the thickest parts of the submarine flanks prevents to identify the horizon B in the FOREVER lines. Note the difference in vertical resolution between the two data sets. (b) Enlargement of the correlation of V between the profiles R4 and FOR20. Inset: Location of the seismic profiles.

the frequency bandwidth of the two seismic data sets (Table 1) results in wavelets of  $\sim 50$  ms wide for the REUSIS data and of 12.5 ms for the FOREVER data. It is therefore difficult to precisely tie reflectors between the two surveys. As few seismic lines were collected beyond the edifice base during the REUSIS cruise and since the configuration used during the FOREVER experiment did not allow penetration of the acoustic signal below the volcanic edifice, correlation of the two seismic data sets can only be performed between a few seismic profiles. However, at existing intersections, it appears that the deeper horizon highlighting in our data (horizon V) correlates with the horizon also named V in the REUSIS interpretations (Figure 8) and considered by de Voogd et al. (1999) as the top of sedimentary units predating the volcanism. TWT time differences at FOREVER-REUSIS crossover are generally less than 0.05 s and of 0.01 s (TWT) at the intersection between the profiles R4 and FOR20 (Figure 8), attesting to the recognition of the same horizon V on the FOREVER seismic profiles. The full coverage of the FOREVER seismic lines enables to extend the location of the horizon V of de Voogd et al. (1999) all around the island (Figure 6a).

Thereafter, we investigate the distribution of the material deposited in the volcaniclastic apron of La Réunion above and between each horizon, in order to identify potential changes in the source(s) of sediment supply during the evolution of the volcanic complex. We then discuss in section 6 the significance of the horizons, together with the nature, origin, and mode of deposition of the seismostatigraphic units with respect to the evolution of the volcanic complex.

## 5. Depth Variations of the Horizons and Thickness Maps

### 5.1. Influence of the Seismic Velocity

Figure 6 shows the extent and TWT time for each horizon. As seafloor topography induces lateral variations of seismic velocity, we also constructed depth maps for the horizons V and S using a seismic velocity of 1,500 m/s in the water column and a higher velocity within underlying material. Unfortunately, the configuration used to collect the seismic data during the FOREVER cruise did not permit to constrain the seismic velocities within the apron. We therefore consider the seismic velocities derived by Charvis et al. (1999) and Gallart et al. (1999) from the OBS data gathered during the REUSIS cruise. An average velocity of 4,000 m/s has been proposed by the authors. Such velocity is well adapted for the volcanic edifice but probably not for the volcanosedimentary units composing the distal part of the apron. We thus present depth-converted maps (Figure S1 in the

supporting information) using a range of seismic velocities from 2,000 m/s to 4,000 m/s within the sediment. A seismic velocity of 2,000 m/s is comparable to the  $P$  wave velocities measured at Site 953 in the volcanoclastic apron offshore Gran Canaria (e.g., Funck & Lykke-Andersen, 1998) and in the Lesser Antilles (e.g., Le Friant et al., 2015). For the thickness of the seismostratigraphic units, there is a linear relationship between the TWT time and the figure in meters. We therefore only discussed the thickness maps in time.

## 5.2. Depth Maps

All maps produced for the horizons V and S show a strong difference between the northern and southern regions (Figures 6a, 6b, and S1). Whatever the seismic velocity used within the apron, the greater depths are always located in the northern region. Deplus et al. (2009) reported the same observation for the basement topography. This observation, together with ours, suggests a control of the basement morphology on the horizons depth. The second feature observed both on the time and depth domain converted maps, is the shallowest area offshore the Piton de la Fournaise, which is present for the horizons V and S (Figures 6a, 6b, and S1).

## 5.3. Thickness Maps

### 5.3.1. Above the Horizon V (From Unit II to Unit IV)

Cumulative isopach map of the units deposited above the horizon V (units II, III, and IV) shows an increase in thickness toward the island, which attests to a material origin from La Réunion (Figure 9a). These units represent the volcanoclastic apron of La Réunion, which extends beyond the edifice base (indicated with the dash circle in Figure 9) up to a distance of about 70 km northward. The thickness increases from 0.20 s TWT in the distal region, with a minimum value of  $\sim 0.10$  s TWT offshore Mauritius, to 0.60 s TWT in the proximal region. The contour map shown in Figure 9a reveals a progressive increase and a regular material distribution centered on Piton des Neiges, as depicted by the subcircular shape of the isopachs. For example, the dash circle, whose center is located on the present-day summit of Piton des Neiges, roughly corresponds to the 0.40 s TWT isoline (transition between the yellow and orange areas). Four local accumulations are, however, observed beyond the edifice base. The largest accumulation ( $v_1$ ) is located in the northern region, while the second and third major accumulations ( $v_2$  and  $v_3$ ) are located in the southeastern and southern regions. Each accumulation shows thicknesses ranging from 0.30 s to 0.35 s TWT. The last accumulation ( $v_4$ ) corresponds to the smallest accumulation identified in our data. It is located in the distal part of the northern region and shows an average thickness of less than 0.30 s TWT. Due to its location, we relate it to the Mauritius Island. Despite the accumulation  $v_4$ , the contribution of Mauritius in supplying material to the volcanoclastic apron of La Réunion appears to be low since the deposition of the horizon V.

### 5.3.2. Between the Horizons V and S (Unit II)

Figure 9b1 shows the thickness distribution of the material deposited around La Réunion between the horizons V and S, which corresponds to the thickness of the unit II (Figures 4, 5, and 7). The thickness is relatively homogeneous in the distal part of the northeastern, southeastern, and southwestern regions, while two major accumulations are observed close to the edifice base. The largest accumulation  $b_1$  is located to the north and shows a thickness that exceeds 0.25 s TWT at the base of the submarine flanks, which slightly decreases to 0.10 s TWT beyond the edifice base. Bedded layers compose the accumulation  $b_1$  (Figures 4b and 10b/10c). The second accumulation  $b_2$  is located in the southeastern region and shows thicknesses ranging from 0.20 s TWT close to the edifice base to 0.10 s TWT beyond. The lateral extent of  $b_2$  is restricted within a broadly round shape, which contrasts with the widespread extent of  $b_1$ . Bedded layers also compose the accumulation  $b_2$  and are particularly well observed in the distal part of the accumulation (Figure 10d). The rough and chaotic terrains that characterize the submarine flank, together with the presence of highly disrupted reflections below, obscure the interpretation of the seismic facies that constitute the central part of  $b_2$ . Nevertheless, we can clearly identify in places discontinuous bedded reflections indicating the presence of stratified material in the central area, attesting to a deposition due to gradual dismantling. Four smaller accumulations named  $b_3$ ,  $b_4$ ,  $b_5$ , and  $b_6$  are observed locally. Each accumulation displays bedded ( $b_3$ ) to well-bedded ( $b_6$ ) layers, except the accumulations  $b_4$  and  $b_5$ , which exhibit, respectively, highly (proximal area; Figure 3c) to slightly (distal area) disrupted reflections and a thin chaotic facies underlain by bedded reflections (Figure 10a). Despite this thin chaotic facies, the seismic signatures recognized within these small accumulations also attest to a deposition due to gradual dismantling.

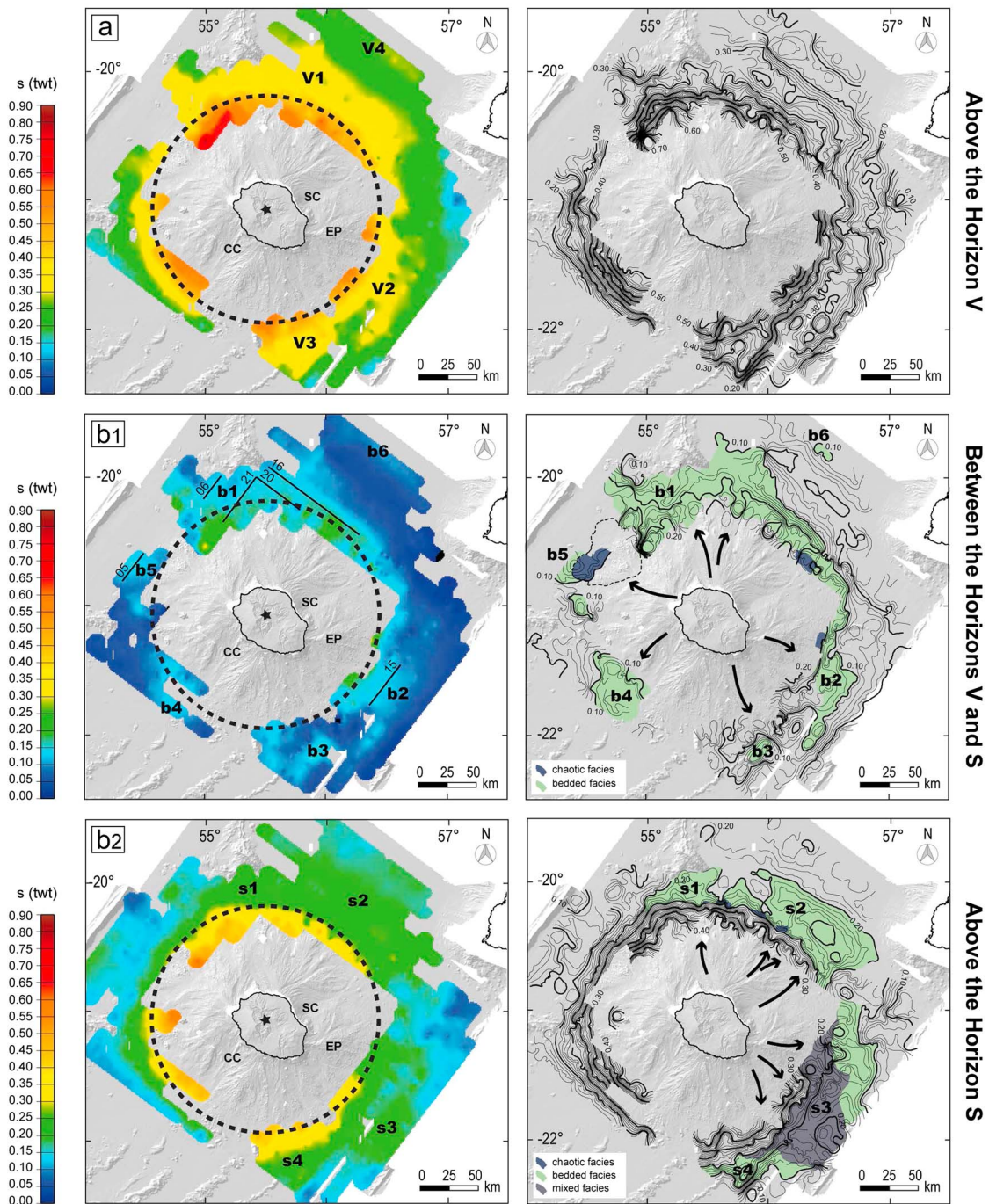


**Figure 9.** Thickness distribution of material deposited offshore La Réunion superimposed on shaded bathymetry (left column). (a) Above the horizon V (i.e., cumulative thickness of the units II, III and IV). Dashed circle, the center of which is shown by a star, indicates the base of the volcanic complex. (b<sub>1</sub>) Between the horizons V and S (i.e., unit II) and (b<sub>2</sub>) above the horizon S (cumulative thickness of the units III and IV). (c<sub>1</sub> to d<sub>2</sub>) During the most recent building periods of the volcanic complex, respectively, offshore the northern and southeastern regions. (e<sub>1</sub> and e<sub>2</sub>) Detailed evolution in the southeastern region. Contour lines of the thickness distribution of material deposited offshore La Réunion superimposed on shaded bathymetry (right column). Main contour lines are of 0.05 s (TWT). Dashed lines in the northwestern region delimit the front instability recognized by Le Friant et al. (2011). The colors on the isopach maps indicate the extent of bedded to well-bedded facies (light green), chaotic facies (dark blue) and a combination of chaotic to highly disturbed seismic facies (gray). Seismic profiles 05, 06, 20-21, and 15 are illustrated in Figure 10, while the profile 16 is illustrated in Figure 4b. CC: Cilaos Canyon. SC: Salazie Canyon. EP: Eastern Plateau. Color bar scale is slightly different for e<sub>1</sub> to e<sub>2</sub>, to better identify the pattern of the material distribution during these recent time intervals.

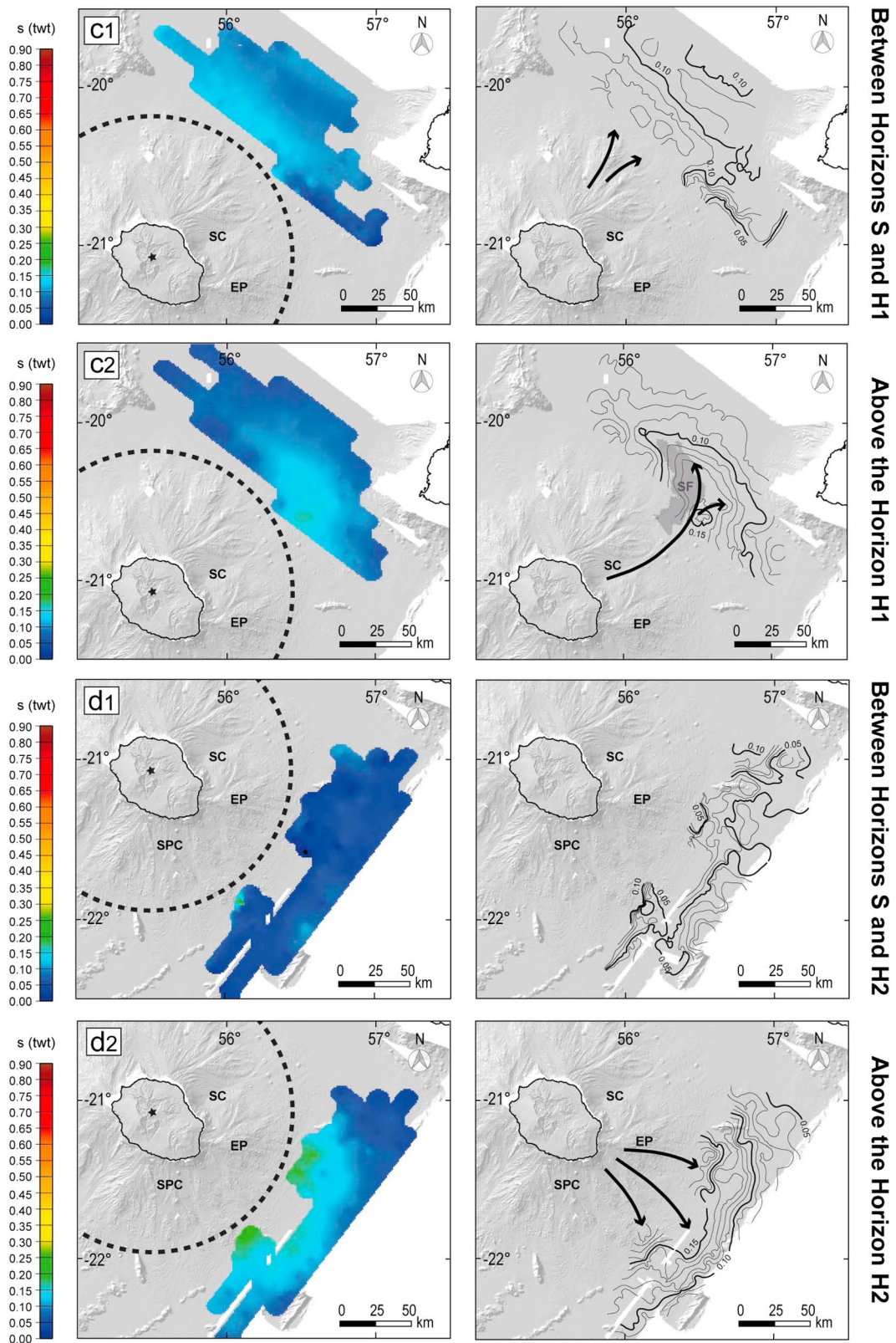


Figure 9. (continued)

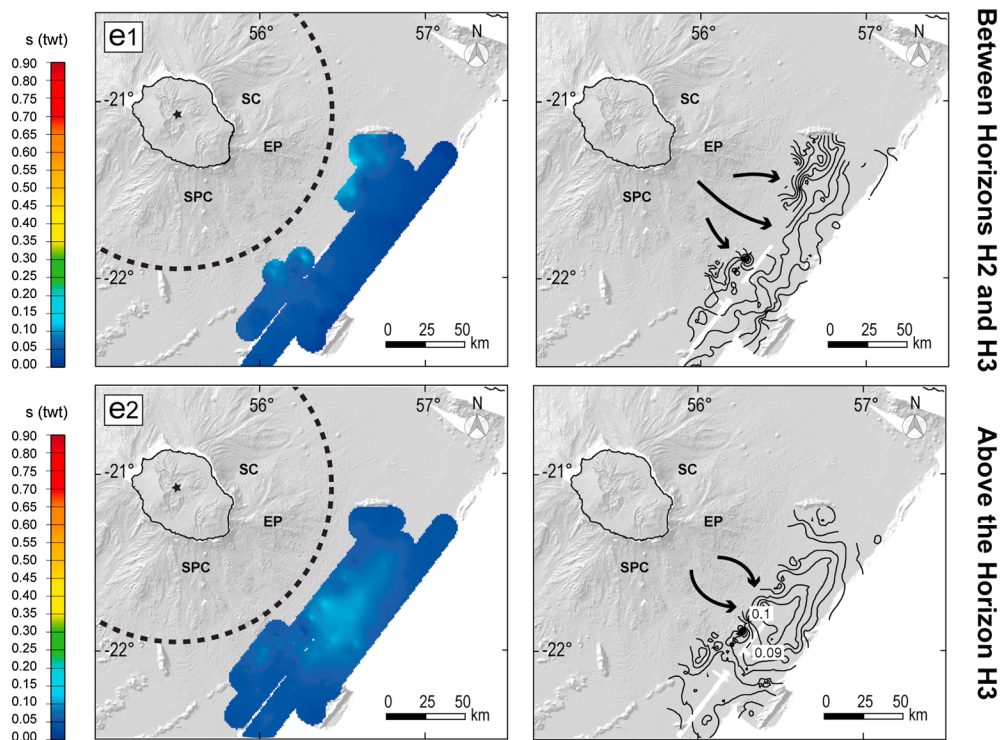


Figure 9. (continued)

**5.3.3. Above the Horizon S (From Unit III to Unit IV)**

Material deposited above the horizon S and beyond the edifice base mainly accumulates in the northeastern and southeastern regions (Figure 9b2). A progressive and regular increase in the material thickness centered on the summit area of Piton des Neiges is depicted by the subcircular shape of the isopachs. Minimum thickness (<0.10 s TWT) is recognized south of Mauritius. The accumulations identified in the northeastern and southeastern regions may be divided up into subzones that we call  $s_1$ ,  $s_2$ ,  $s_3$ , and  $s_4$ . The average thickness in each area decreases from 0.25 s TWT at the edifice base (exceeding 0.40 s TWT in the subzone  $s_4$ ) to 0.10 s TWT in the distal areas. Thicknesses measured in these subzones are approximately twice as high than those measured in the western region. It is interesting to note that each subzone extends up to ~50 km from the edifice base, with the exception of the subzone  $s_1$ , which only extends ~35 km away. The extent of the subzone  $s_1$  is limited by the presence of the volcanic feature identified in Figure 3a, which may have acted as barrier to sediment migration further north. Of particular interest is the widespread extent of a chaotic facies in the eastern region (Figure 10e), which almost entirely covers the surface area of the subzone  $s_3$  (Figure 9b2). The chaotic facies can be mapped until the Mauritius Fracture Zone, approximately 55 km from the edifice base.

**5.3.4. Between the Horizons S and H<sub>1</sub>, and Above H<sub>1</sub> (NE Region)**

Material continues to accumulate in the northern region between the horizons S and H<sub>1</sub> (Figure 9c1) and displays well-bedded seismic reflections in the distal area (Figure 4a), slightly disturbed locally in the proximal area (Figure 4b). Above the horizon H<sub>1</sub> (unit IV; Figure 4), material accumulates in a different area: offshore the canyon of Salazie (Figure 9c2). Material thickness exceeds 0.16 s TWT in the central part of the accumulation to regularly and progressively decrease to 0.12 s TWT at the edges, while it is ~0.08 s TWT elsewhere. The shape of the isopachs allows to trace back the source of the material supply to the canyon of Salazie. Well-bedded seismic reflections, similar to the ones observed in unit III (Figure 10c) and defining the bedded facies shown in Figure 9b1 (green areas), characterize the accumulation, while a semitransparent facies with wavy to sub-horizontal, parallel internal reflections of moderate amplitudes defines the surrounding areas (Figure 4).

**5.3.5. Between the Horizons S and H<sub>2</sub>, and Above H<sub>2</sub> (SE Region)**

**5.3.5.1. Between the Horizons S-H<sub>2</sub> and Above H<sub>2</sub>**

Half volume of material accumulated in the southeastern region between the horizons S and H<sub>2</sub> than in the northeastern region between S and H<sub>1</sub> (Figure 9d1 compared to Figure 9c1). Material mean thickness is about

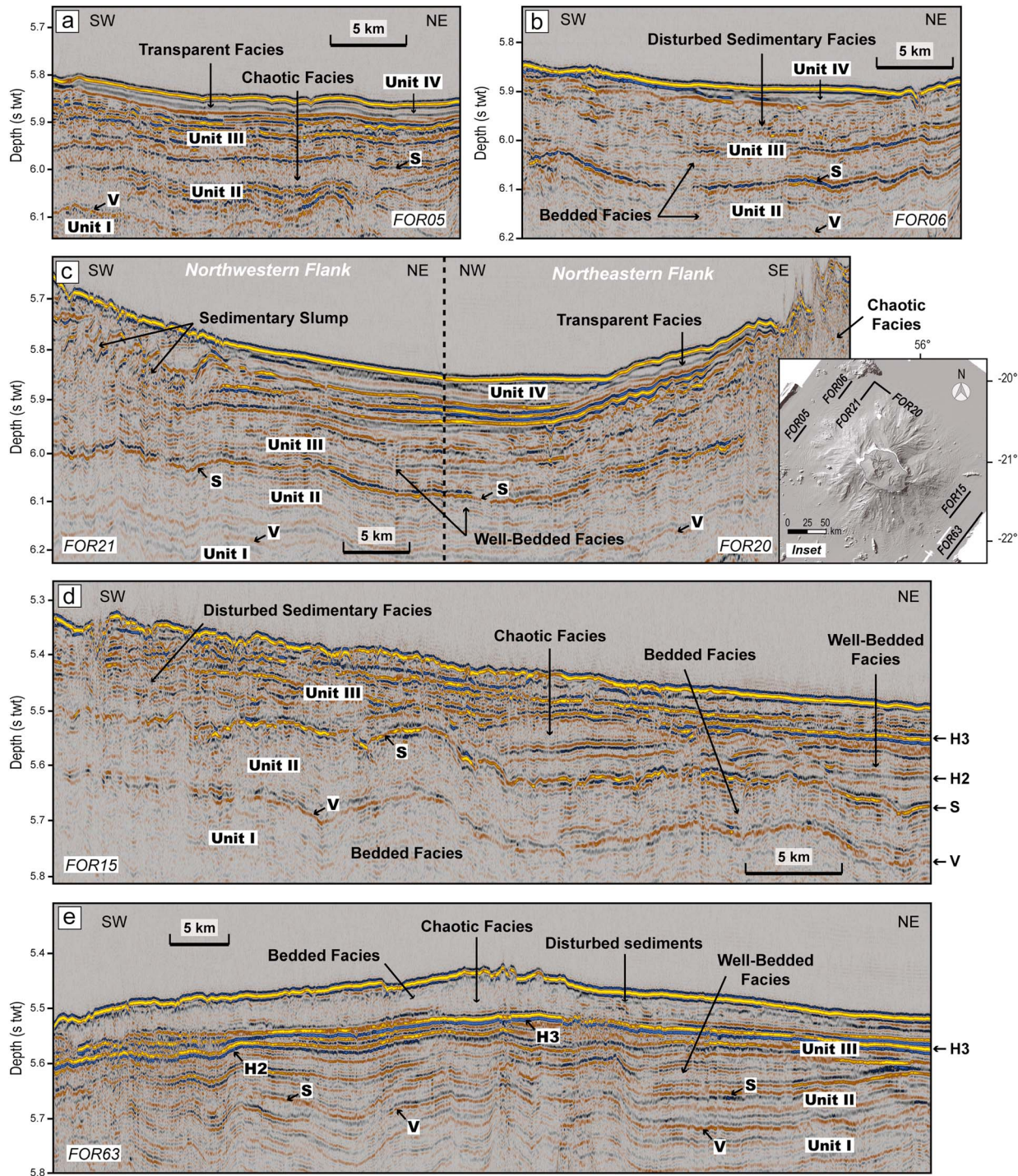


**Figure 10.** Seismic profiles (a) FOR05, (b) FOR06, (c) FOR21-FOR20, (d) FOR15, and (e) FOR63 illustrating the seismic signature of the material composing, respectively, the accumulations  $b_5$ ,  $b_1$ ,  $b_1$ ,  $b_2$ , and offshore  $b_2$ . Inset: Location of the seismic lines presented here.

0.05 s TWT and small accumulations of  $\sim 0.09$  s TWT thick are only observed near the Mauritius Fracture Zone. Bedded and well-bedded seismic reflections characterize the material deposited between S and  $H_2$  (Figure 10d).

Above the horizon  $H_2$ , twice as much material accumulated in the southeastern region than between S and  $H_2$  (Figure 9d2 compared to Figure 9d1). A progressive and regular decrease toward the Mauritius Fracture

Zone is shown by the isopachs. Material thickness reaches 0.15 s TWT at the edifice base, up to 0.19 s TWT offshore the Eastern Plateau, to slightly decrease to 0.10 s TWT toward the distal region. Well-bedded seismic reflections directly lie on the horizon  $H_2$  (Figure 10d) and are clearly identified in the distal region. These well-bedded reflections are overlain by a chaotic facies (Figure 10e), which was interpreted by Le Friant et al. (2011) as a mass-wasting deposit, whose maximum thickness reaches  $\sim 0.09$  s TWT in the central area. Another chaotic facies of about 0.02 s TWT thick, older than the aforementioned deposit, is observed directly over  $H_2$  (Figures 7 and 10d). This deposit is covered by disturbed seismic reflections.

Unfortunately, we were not able to trace the horizon  $H_2$  to the southern region, preventing investigation of the subzone  $s_4$  (Figure 9b2).

#### 5.3.5.2. Between the Horizons $H_2$ - $H_3$ and Above $H_3$

Another prominent reflector is observed above the horizon  $H_2$  and widely recognized in the southeastern region, covering an area comparable to that of the horizon  $H_2$  (Figures 6e, 7, and 10d and 10e). This strong reflection, referred to as horizon  $H_3$ , is particularly well observed in the distal region where it marks in places the base of the mass-wasting deposit described by Le Friant et al. (2011) (Figure 10e). Thickness of material deposited between the horizons  $H_2$  and  $H_3$  varies from approximately 0.10 s TWT close to the edifice base to 0.03 s TWT in the distal part (Figure 9e1). Above the horizon  $H_3$ , material mostly concentrates in the central part of the southeastern region, as shown by the contour lines in Figure 9e2. A maximum thickness of 0.10 s TWT is observed on the isopach map.

## 6. Discussion

The FOREVER seismic data set has provided a unique opportunity to image La Réunion volcanoclastic apron in detail, highlighting the presence of prominent horizons at a local ( $H_1$ ,  $H_2$ , and  $H_3$ ) and at a regional scale ( $V$  and  $S$ ). Hereinafter, we discuss the significance of the horizons, along with changes in material distribution during the time intervals defined by the horizons, with respect to the main building phases of La Réunion volcanic complex.

### 6.1. Significance of the Horizons $V$ and $S$

The horizon  $V$  was first recognized by de Voogd et al. (1999) on the seismic reflection data gathered during the REUSIS cruise. On all the profiles, they identified two major units between the sea bottom and the top of the oceanic crust that can be distinguished by their seismic signature (Figure 8). They related the reflective character of the lower unit, which lies directly on top of the oceanic crust, to oceanic sediment that predates the volcanic edifice, while they interpreted the upper sequence as the volcanoclastic edifice, a term which includes everything that was deposited regardless of the processes involved (lava flows, mass wasting, and sedimentation). The horizon  $V$  marks the boundary between these two units and was thus interpreted by de Voogd et al. (1999) as a stratigraphic marker of the base of La Réunion volcanic edifice.

More recently, another interpretation of the horizon  $V$  has been proposed by Gailler and Lénat (2010). On the basis of morphological correlations between the volcanic constructions inferred from magnetic modeling and the topography of the horizon  $V$  given by de Voogd et al. (1999) from the REUSIS seismic data, the authors interpreted the horizon  $V$  as the top of two buried, still coherent, parts of La Réunion volcanic edifice. However, such interpretation exclusively relies on morphological correlation between their magnetic model and the depth-converted map of the horizon  $V$  shown by de Voogd et al. (1999). This map was produced using a constant seismic velocity of 4,000 m/s below the sea bottom. As pointed out by de Voogd et al. (1999), the choice of a constant velocity for the "volcanoclastic edifice" may introduce artifacts if lateral velocity variations are present, a higher velocity leading to a pull-up effect on the topography of the horizon. Therefore, the presence of buried, coherent parts inside the edifice, as deduced from the magnetic modeling of Gailler and Lénat (2010) may explain the topographic bulges observed in the depth-converted map of the horizon  $V$  shown by de Voogd et al. (1999), without making  $V$  the top of these coherent volcanic parts.

Identification of the horizon  $V$  on the FOREVER seismic lines (this contribution; see the correlation with the horizon  $V$  of de Voogd et al. (1999) on Figure 8) enables to extend its location all around the volcanic edifice, at great distance from the base (up to  $\sim 70$  km in the northern region; Figure 6a). The horizon  $V$  therefore represents a stratigraphic marker of a major event that occurred at the scale of the surrounding basin. The cumulative isopach map we have constructed for the units deposited above the horizon  $V$  (Figure 9a)



clearly shows an increase in the thickness toward the island, attesting to an origin of the material from La Réunion. Furthermore, the horizon V corresponds to the top of the basal unit (I), which displays relatively low-amplitude reflections. Unit I was already identified on the REUSIS seismic lines and imaged below the edifice base, draping the oceanic basement (see Figure 8 in de Voogd et al., 1999). Due to its reflective character, it has been interpreted by de Voogd et al. (1999) as the oceanic sediment preceding La Réunion volcanism. A similar interpretation for the basal units identified on the seismic profiles offshore Hawaii and the Canary Islands, which display similar patterns, was given by Rees et al. (1993) and Urgeles et al. (1998), respectively. It is also noteworthy that V displays a reverse polarity when compared to the sea bottom reflection, supporting a velocity or a density inversion (de Voogd et al., 1999; our data). All these observations are in agreement with the interpretation of the horizon V as a stratigraphic marker of the onset of La Réunion volcanism in the surrounding basin. Hereafter, we discuss how the onset of the volcanism may produce a significant horizon.

Staudigel and Clague (2010) present a model for the growth of seamounts and volcanic islands on the oceanic crust. At the beginning, the seamount grows on the seafloor through continuing eruptions of pillow lavas. With decreasing depth, the pillow lavas become more vesicular and interlayered with pillow breccias, debris flows, and hyaloclastites. When the seamount summit reaches shallow depth, significant degassing of magmatic volatiles takes place causing explosive activity. It is unlikely that the horizon V marks the very onset of La Réunion volcanism, since it is thought to consist in emission of densely packed and nonvesicular pillow lavas that will constitute the core of the seamount. V may be better explained by the onset of the submarine explosive activity, since material may extend far beyond the seamount core. Explosive pyroclastic activity at West Mata Volcano provided evidence that such activity can also affect basaltic systems without necessarily requiring extraordinary initial contents or accumulation of volatiles (Clague et al., 2011). The depth at which submarine explosive activity may start is not precisely defined. Staudigel and Clague (2010) indicate a water depth of ~700 m below sea level (mbsl), but numerous observations suggest that Strombolian basaltic eruptions also occur at greater depths: between 500 and 1,750 mbsl along the Mid-Atlantic Ridge (Eissen et al., 2003), but also as deep as 2,200 mbsl at West Mata Seamount in the Lau Basin (Clague et al., 2011). Widespread distribution of pyroclastic deposits blanketing axial valleys have also been previously reported at 3,800 m deep on the Gorda Ridge, in the Pacific Ocean (Clague et al., 2009), and at 4,000 m deep on the Gakkel Ridge, in the Arctic Ocean (Sohn et al., 2008); these two ridges being volatile-poor mid-ocean ridge basalt systems.

In conclusion, we interpret the horizon V as a stratigraphic marker of the onset of the submarine explosive activity, an early stage in the growth of La Réunion volcanic edifice. Such interpretation is slightly different from the one of de Voogd et al. (1999), as V does not correspond to the base of the volcanic edifice *sensu stricto*. In fact, neither of the two interpretations are contradictory. A careful look at the third stage of the model of the seamount growth proposed by Staudigel and Clague (2010) clearly shows that, both, the base of the seamount and the base of the unit resulting from the submarine volcanic explosive activity lie on top of preexisting oceanic sediment and merge at the foot of the seamount flanks. Thus, beyond the edifice base, the horizon V corresponds, at the same time, to the top of the preexisting oceanic sediment and to the onset of the submarine volcanic explosive activity.

The horizon S has also been identified all around the volcanic edifice on the FOREVER seismic lines, at great distance from the base (Figure 6b). It is younger than V and thus indicates a major, intermediate phase in the growth of the volcanic complex. We will discuss in section 6.4.2 that it could mark the onset of the growth of the present Piton des Neiges.

## 6.2. Overall Morphology of the Active Volcanic Complex Through Time

Sea bottom morphology analysis performed by Le Friant et al. (2011) showed that the base of the volcanic complex (defined as the slope transition between the volcanic complex and the surrounding seafloor) could be approximated by a circle with a radius of ~100 km (dash circle in Figure 3a), which contrasts with its elongated subaerial form. In addition, the center of the circle is located at the central area of Piton des Neiges, suggesting that this edifice was the main volcano on which evolved the entire complex of La Réunion. A first order analysis of material distribution in the volcanoclastic apron of La Réunion through time strengthens this interpretation. Indeed, the material distribution above the horizons V and S (Figures 9a and 9b2) reveals a progressive and regular increase in the units thickness toward the central area of Piton des Neiges, at any time. The subcircular shape of the isopachs, together with this progressive and regular pattern, suggests

the existence of a single, major source of material supply centered on Piton des Neiges during the whole evolution of the volcanic complex. The sedimentary record does not support the existence of another volcano comparable in size and lying beside the Piton des Neiges as suggested for Les Alizés volcano (e.g., Gailler & Lénat, 2010; Lénat et al., 2001; Oehler et al., 2004, 2008; Smietana, 2011). Such a configuration (see Figure 3 in Oehler et al., 2008) would have led to different isopach patterns displaying an elliptical shape or even an “8” shape, consistent with two distinct material supply sources comparable in dimension. The lack of evidence of Les Alizés volcano in the present-day morphology of the volcanic complex, as well as in our seismic data, leads us to ascribe a much smaller size for Les Alizés volcano comparable to that of Piton de la Fournaise.

### 6.3. Gradual Degradation/Dismantling Versus Catastrophic Flank Collapses

From interpretation of bathymetric and acoustic data available prior to 2006, Oehler et al. (2004, 2008) concluded that La Réunion submarine flanks were built from accumulation of landslide deposits, mainly of debris avalanche type. However, the data collected prior to 2006 solely covered parts of the submarine flanks, the other ones being only constrained by few isolated profiles.

The FOREVER cruise, carried out in 2006, provided a complete coverage of La Réunion submarine flanks and surrounding abyssal plain (Figure 2).

Joint analysis of the data (bathymetric and acoustic) enabled Le Friant et al. (2011) to characterize La Réunion submarine flanks as rough and chaotic terrains. Offshore Piton de la Fournaise, these terrains extend onto the abyssal plain: a speckled pattern—typical of debris avalanche deposits—is visible on the reflectivity map (see Figure S2 in Le Friant et al., 2011) and a widespread chaotic unit is recognized in the seismic data beyond the edifice base (Figure 10e). It is not the case offshore Piton des Neiges, indicating that the rough and chaotic terrains ended at the base of the submarine flanks. These observations led Le Friant et al. (2011) to propose two distinct behaviors for the volcanoes. The Piton des Neiges would be affected by slow deformation processes such as sliding or spreading. The authors explained the chaotic texture of the submarine flanks as the result of these slow deformation processes that continuously dismantled the flanks of Piton des Neiges, leading to the formation of numerous secondary slope instabilities. To the contrary, Piton de la Fournaise—formed on a preexisting edifice—collapsed several times toward the sea, generating large debris avalanches that flowed down onto the abyssal plain.

Until recently, chaotic units observed in seismic data over the abyssal plain were interpreted as debris avalanche deposits resulting from large, catastrophic flank collapses that affected the surrounding volcanic islands (Deplus et al., 2001; Le Friant et al., 2003; Urgeles et al., 1997). The Integrated Ocean Drilling Program Expedition 340 carried out offshore the Lesser Antilles provided for the first time evidence for the composition and origin of such chaotic units offshore Montserrat and Martinique Islands. The seismically chaotic deposits were successfully drilled and exclusively recovered seafloor sediment (including mud, tephra layers, and turbidites), revealing a complete lack of volcanic debris avalanche deposits (Brunet et al., 2015; Le Friant et al., 2015). Le Friant et al. (2015) interpreted these “seismically chaotic facies” deposits as resulting from widespread deformation of pre-existing sediment on the abyssal plain, triggered by the emplacement of debris avalanche deposits on the edifice flank. A closer look at the chaotic unit in the seismic data offshore Piton de la Fournaise (Figure 10e) shows the presence of undisturbed to slightly deformed seismic reflectors, alternating with a chaotic facies. These observations, along with the new Integrated Ocean Drilling Program findings of the Expedition 340, lead us to reinterpret this “chaotic” deposit as widespread, deformed, pre-existing seafloor sediment resulting from the emplacement of the Piton de la Fournaise debris avalanche deposits on the submarine flank, where hummocky terrains were previously observed (Le Friant et al., 2011; Lénat et al., 1989; Oehler et al., 2004, 2008). Therefore, chaotic units observed in seismic data on the abyssal plain do not necessarily correspond to debris avalanche deposits as commonly and previously thought. However, they may be regarded as evidence of large flank-collapse events that affected the surrounding volcanic islands.

The absence of widespread chaotic units offshore Piton des Neiges, beyond the edifice base, suggests that no large debris avalanche deposits flowed down the submarine flanks of Piton des Neiges, despite the chaotic texture of its submarine flanks. Seismic investigation in the volcanoclastic apron of La Réunion shed light on a prevailing of gradual degradation/dismantling processes on large, catastrophic flank collapses, as previously suggested by Salvany et al. (2012) from on-land studies.

#### 6.4. New Model of Evolution for La Réunion Volcanic Complex

Isopach mapping of material deposited above the horizon V (Figure 9a) reveals La Réunion volcanic edifice as the main source of material from the onset of La Réunion volcanism. The minimal amount of material related to Mauritius Island above the horizon V indicates that the main building phases of La Réunion occurred after the ones of Mauritius (i.e., <7–8 Ma). Recognition of a discordance of the horizon V on the Mauritius flanks is in agreement with this interpretation (de Voogd et al., 2009; our data).

##### 6.4.1. From the Submarine Edifice to an Emergent Island (From V to S)

###### 6.4.1.1. Construction of a Protoedifice

Direct observations of explosive submarine eruptions, and syneruptive transport and deposition of related products, are rare. To date, only the submarine eruptions of the NW-Rota-1 submarine volcano in the Mariana Arc (Walker et al., 2008) and the West Mata volcano in the Lau Basin (Clague et al., 2011) have been observed directly. In their contribution, Walker et al. (2008) reported on the nature, distribution, and dispersal of volcanoclastics during ongoing submarine eruptions at NW-Rota-1, from 2003 to 2006. The authors documented two mechanisms of transport for the eruptive products: (1) gravitational collapses of the eruptive column, generating plumes at multiple depths and in all directions, transporting volcanoclastic material down the flanks several kilometers away, and carrying fine ash layers up to tens of kilometers from the summit; and (2) landsliding of recent ejecta accumulating near the active vents, becoming unstable and collapsing periodically. At West Mata Volcano, volcanic sand almost entirely composed the lower slopes of the volcano and mostly represented fall deposits from lava fountains and pyroclastic-rich plumes from nearby eruptions (Clague et al., 2011). Pillow breccia have also been reported near the plateaus and interpreted as resulting from fragmentation of pillow lavas flowing down the steep slopes of the upper flanks.

We can assume that similar processes have affected La Réunion seamount during its submarine explosive activity, leading to the production and widespread dispersal of volcanoclastics in the surrounding environment. Volcanoclastic deposits may have partly accumulated near the vents (bombs and lapilli), down the slopes (sand), or delivered in the distal environment (ash), landsliding and reworking contributing to further disperse these volcanoclastics toward the distal regions.

The study undertaken by Romagnoli and Jakobsson (2015) on the volcanic island of Surtsey in the Vestmannaeyjar archipelago, underlined the importance of subaerial and submarine erosion—during and after—the emergence of the volcanic island. This constant and rapid erosion at an island's emergence was also discussed by Washington (1909) at Graham Island in the Mediterranean Sea, which was eroded and leveled by wave action, before to completely disappear 6 months after its appearance. From examination of an ODP drilling core at Site 953, Carey et al. (1998) also underlined a rapid flux of volcanoclastic material to the marine environment during the emergence of Gran Canaria, concluding that high eruptive activity may have occurred during that time, both in the submarine and subaerial environments. We thus consider that most of the material deposited between V and S (unit II) reflects the submarine explosive activity of La Réunion seamount as well as the submarine and subaerial erosion and activity of the emergent island. Observations to the north of the largest accumulation  $b_1$  (Figure 9b1) led us to consider that the central area of the emergent island was probably slightly located to the north from the current location of the summit of Piton des Neiges (black star in Figure 9). This interpretation is supported by a recent on-land study performed by Berthod et al. (2016), which locates the magma chamber of an "initial Piton des Neiges", 4 km north to the current summit of Piton des Neiges. The presence of local accumulations to the south ( $b_3$ ), southwest ( $b_4$ ), and west ( $b_5$ ) (Figure 9b1) suggests a size relatively important for the emergent island and the whole volcanic edifice is named hereafter, proto-Piton des Neiges. Prevalence of bedded to well-bedded seismic reflections between the horizons V and S indicates gradual degradation/dismantling and fallout deposition as continuing processes during the submarine growth and the emergence of the proto-Piton des Neiges. Chaotic facies observed in the proximal region (Figure 9b1) suggests punctual occurrences of slumping and sliding processes due to oversteepening, for instance.

###### 6.4.1.2. A Major Instability Affecting the Protoedifice?

The accumulation  $b_2$  corresponds to the second large accumulation identified between the horizons V and S (Figure 9b1). The confined distribution of the material within  $b_2$ , marked by the lobe shape of the contour lines, clearly contrasts with the widespread extent of the accumulation  $b_1$ . Another point of interest and of particular significance is the coincidence between the location of (1) the highest thickness within the accumulation  $b_2$ ; (2) the shallowest depth of the horizon S (Figures 6b and S1d to S1f); and (3) the

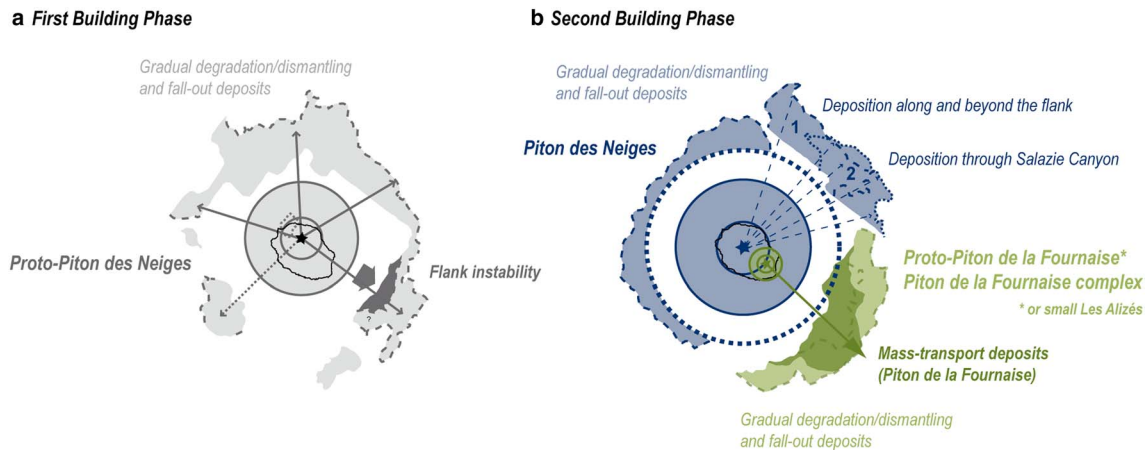


**Figure 11.** Model of evolution of La Réunion volcanic complex since the onset of the volcanism during the (a) first and (b) second building phases determined from our data. (1) Deposition along and beyond the flank. (2) Deposition through Salazie Canyon. The present-day shoreline of the island is shown in black and mass-wasting events represented by dark colors.

undulated morphology of the horizon S, which is only observed in the southeastern region (Figures 7 and 10d). A relationship between these three features may exist and prove to be specific to the southeastern region, since such a relationship is not observed for the accumulation  $b_1$  (Figures 6b and 9b1). We have investigated the seismic signature of the accumulation  $b_2$  to better understand and characterize its origin. Bedded to well-bedded seismic reflections define the accumulation  $b_2$  in the distal environment (cyan areas in Figure 9b1), which may mainly reflect deposition of material originating from gradual degradation/dismantling and fallout processes. To the contrary, the area delimited by the subrounded contour lines in the proximal region (green areas in Figure 9b1) is characterized by a chaotic facies. Comparing with current interpretations (e.g., Le Friant et al., 2011), and based on similarities observed with the present-day morphology of the eastern submarine flank, we interpret the wavy character of the horizon S as reminiscent of buried sediment waves forming by deposition from turbidity currents over rough and chaotic preexisting terrains. Similitudes between the morphology of the horizon S and a seismic reflection related to buried sediment waves offshore Borneo, in Indonesia, strongly supports our interpretation (see Figure 12a in Posamentier & Kolla, 2003). From the seismic signature of the material composing the accumulation  $b_2$ , together with the lobe shape of the contour lines, we suspect the chaotic facies recognized in the proximal area corresponds to a mass-wasting deposit resulting from a large instability that affected the southeastern flank of the proto-Piton des Neiges (Figure 11a). This flank instability would have partially formed the accumulation  $b_2$  in the proximal region and favored subsequent development of sediment waves by turbidity currents. The wavy character of the horizon S could also be explained as resulting from compressive strains on the sediment at the front of the advancing mass-wasting deposit, as suggested by Oehler et al. (2008) to explain the presence of sediment waves around La Réunion. Both processes are in agreement with the occurrence of a large mass-wasting event.

An alternative interpretation of the accumulation  $b_2$  would be to consider it as reflecting the activity of a second volcanic vent, which would have been contemporaneous to the volcanic activity of the proto-Piton des Neiges. Direct observations of submarine explosive eruptions and well-documented eruptions of recently-formed volcanic islands showed that several vents can be active at the same time during the submarine volcanism stage (e.g., Clague et al., 2011; Schnur et al., 2017) or at the emergence of the island (e.g., Romagnoli & Jakobsson, 2015). A second volcanic vent could correspond to Les Alizés volcano, assuming a very small size for this volcano. However, the presence of a chaotic facies in the proximal part of the accumulation  $b_2$ , along with the lobe shape of the isopachs, are more in favor of a mass-wasting deposit. We therefore prefer the first interpretation considering the accumulation  $b_2$  as resulting from a flank instability that affected the proto-Piton des Neiges.

**6.4.2. From the Mature Island Stage to the Erosional Stage (From S to Present)**

Above the horizon S, material deposited offshore accumulated all around the volcano. Isopach distribution of material (yellow area on Figure 9b2) underlines the existence of a single, major source of material supply

during this time interval: the Piton des Neiges. Thereby, the horizon S can be regarded as a stratigraphic marker of the onset of the Piton des Neiges volcanic activity. The oldest subaerial lava flows identified on La Réunion Island have been aged to 2.17 Ma (Quidelleur et al., 2010) and found in La Montagne Massif (Figure 1b). If we assume La Montagne Massif to represent the remnants of the proto-Piton des Neiges, as proposed earlier by Gillot et al. (1994) and Salvany et al. (2012), the horizon S is younger than 2.17 Ma, and an age of 1.4 Ma can be inferred for the horizon S. But if we consider La Montagne Massif as a first expression of the Piton des Neiges volcanic activity, an age older than 2.17 Ma is presumed for this horizon.

Following previous seismostratigraphy studies (Leslie et al., 2002; Rees et al., 1993; Urgeles et al., 1998), our observations allow us to interpret the two seismic units above the horizon S as reflecting the main building phases of the volcanic complex (i.e., subaerial stage; unit III) and its erosional stage (unit IV). The absence of unit IV in the southeastern region is directly related to the young age and still ongoing volcanic activity of Piton de la Fournaise (i.e., erosional stage not reached yet).

Beyond the base of the volcanic complex, material mainly deposited on the eastern part, with two large accumulations observed at the northeast ( $s_2$ ) and at the southeast ( $s_3$ ) (Figure 9b2). These accumulations are directly located offshore the northeastern flank of Piton des Neiges ( $s_2$ ) and the eastern flank of Piton de la Fournaise ( $s_3$ ), which are exposed to dominant winds and heavy rainfall. La Réunion's tropical climate is indeed characterized by trade winds having a mean direction from ESE throughout the year, leading to a strong asymmetry in the rainfall distribution with 1,000 to 2,000 mm/yr on the west side and up to 8,000 mm/yr on the east side (see Figure 1 in Desvars et al., 2011). As already pointed out by Salvany et al. (2012), the northeastern slopes of Piton des Neiges are deeply incised whereas the western slopes are more even and better preserved, which is directly an effect of this asymmetry in the climatic regime. Another effect could be the formation of a striking feature in the upper northeastern submarine flank of Piton des Neiges. There is a wide, smooth depression, named the NE Sedimentary Zone by Oehler et al. (2004) as it corresponds to an undisturbed region of sedimentation (see location in Figure 3a). The absence of large mass-wasting deposits offshore the depression leads us to propose that its formation mainly results from recurrent on-land and submarine erosion, enlarging and deepening it. We therefore suspect that the accumulation  $s_2$  mainly reflects erosion that markedly affects the eastern part of the island. The southeastern accumulation  $s_3$  is also partly related to the presence of the Piton de la Fournaise volcano and will be discussed later.

#### 6.4.2.1. Detailed Evolution of the Northeastern and Southeastern Regions

The presence of two local, prominent horizons in the northern ( $H_1$ ) and southeastern ( $H_2$ ) regions allows a detailed investigation of the evolution of the volcanic complex during this time interval. The chronostratigraphic relationship between the two horizons suggests an age relatively younger for the horizon  $H_2$  than for the horizon  $H_1$ .

Between the horizons S and  $H_1$ , material continues to deposit widely offshore the northeastern area (Figure 9c1), in a similar way that between the horizons V and S (Figure 9b1). While material continues to pile up along and beyond the submarine flank between S and  $H_1$ , material directly accumulates offshore the current canyon of Salazie above the horizon  $H_1$  (Figure 9c2). Excavation of large central depressions named "cirques" in La Réunion began 430 ka ago (Salvany et al., 2012). Since then, successive excavations of deep erosion cirques occurred, with the formation of the paleocirque of Marsouins, of the Plaine des Palmistes, and of the paleocirque and current cirque of Salazie (Figure 1b). It is worth to note that the outlets of each cirque are connected to the canyon of Salazie, through the NE Sedimentary Zone (Figure 3a). It is therefore possible to assume that eroded material originated from the cirques have contributed to feed the accumulation shown in Figure 9c2. This leads to interpret the depression hosting the NE Sedimentary Zone and later on, the canyon of Salazie, as preferential transport paths for on-land eroded material since  $H_1$ . An age as old as 430 ka can thus be inferred for the horizon  $H_1$ .

Between S and  $H_2$  (which is younger than  $H_1$ ), half volume of material than between S and  $H_1$  accumulated in the southeastern region (Figure 9d1), suggesting that less erosion has affected this area. We propose that fewer amount of material deposited is related to the construction of a new volcanic edifice. Above the horizon  $H_2$ , material deposited is twice more important than between S and  $H_2$  (Figure 9d2 compared to Figure 9d1). The horizon  $H_2$  can be interpreted as marking the emergence of the new volcano, as the rate of erosion is more important in subaerial environment (Mitchell et al., 2003). One can notice that higher amount of material was deposited during the submarine growth and emergence of the proto-Piton des

Neiges (Figure 9b1) than during the construction of this new volcanic edifice (Figure 9d1). This lower sediment supply may be explained by a smaller size of the newly formed volcano. We propose to relate the horizon H<sub>2</sub> to the early stage of the Piton de la Fournaise history or to a small Les Alizés volcano.

Changes in material distribution between the horizons H<sub>2</sub> and H<sub>3</sub> (Figure 9e1) and above the horizon H<sub>3</sub> (Figure 9e2) are also of interest since they provide further information on the evolution of the southeastern region. Indeed, contrary to the widespread distribution of material between the horizons H<sub>2</sub> and H<sub>3</sub>, material deposited above H<sub>3</sub> have been constricted to the central area of the southeastern region. Interestingly, the area coincides perfectly well with the chaotic facies described by Le Friant et al. (2011). An illustration of this chaotic facies is presented in Figure 10e. We propose to interpret the horizon H<sub>3</sub> as marking the initiation of a major flank-collapsing phase that affected the subaerial part of Piton de la Fournaise. The presence of the Eastern Plateau and the large instability to the south might have influenced the distribution of the deposits offshore.

#### 6.4.2.2. The Southern Area

Evolution of the southern accumulation s<sub>4</sub> (Figure 9b2) during the time intervals defined by the horizons S and H<sub>2</sub>, and H<sub>2</sub> and H<sub>3</sub>, could have not been constrained due to the wedging out of the horizon H<sub>2</sub> to the south. However, investigation of the seismic signature of material composing the accumulation s<sub>4</sub> underlines a prevalence of bedded to well-bedded reflectors that we interpret as mainly resulting from erosion and redeposition; the chaotic facies identified in the area (Figure 5, FOR23) is interpreted as resulting from an ancient instability that affected the submarine flank of the volcanic complex during the second building phase.

Two intense periods of erosion affected the southeastern region of the Piton de la Fournaise volcano between 250–220 ka and 150–100 ka, leading to the formation of two paleocanyons of the Rivière des Remparts (Merle et al., 2010). The accumulation s<sub>4</sub> is located offshore the Rivière des Remparts and the Rivière Langevin (Figure 1b). We thus propose that these two intense periods of erosion contributed to feed the accumulation s<sub>4</sub>. However, the proximity of the Saint-Pierre canyon (Figure 3a), together with the thickness of the material deposited within s<sub>4</sub>, suggests that another older, long, and/or intense period of erosion (that affected the Piton des Neiges) likely fed (and initially formed) the accumulation s<sub>4</sub>.

#### 6.4.3. Summary

During the first building phase of La Réunion volcanic complex (i.e., from the horizons V to S; Figure 11a), a proto-Piton des Neiges emplaced. During the submarine growth and the emergence of the protoedifice, gradual degradation/dismantling and fallout processes prevailed and led to the formation of large accumulations offshore. The largest accumulation was identified in the northern region, suggesting that the volcanic center during that period was located slightly further north to the current position of Piton des Neiges. A large instability affected the southeastern flank of the proto-Piton des Neiges, favoring subsequent development of sediment waves by turbidity currents. The horizon S marks the end of the first building phase and denotes the onset of the Piton des Neiges volcanic activity.

During the second building phase (i.e., above the horizon S; Figure 11b), the Piton des Neiges emplaced. Intense erosion affected the Piton des Neiges volcano, leading to the formation of the large depression identified on the upper northeastern submarine flank, hosting nowadays the NE Sedimentary Zone (Figure 3a), and to the accumulation offshore the canyon of Salazie. In between, a proto-Piton de la Fournaise or a smaller Les Alizés volcano emplaced on the southeastern flank of Piton des Neiges. The Piton de la Fournaise emplaced later on and experienced large flank collapses.

## 7. Conclusions

The FOREVER seismic data set has provided a unique opportunity to image La Réunion volcanoclastic apron in detail, enhancing our current understanding on the growth, emergence, and evolution of oceanic intraplate volcanoes.

Four seismostratigraphic units have been identified and interpreted as sediment predating La Réunion volcanism (unit I), material reflecting the submarine volcanic activity of the seamount as well as the emergence of the island (unit II), the main building phases of the volcanic complex (unit III), and the erosion stage that currently affects the Piton des Neiges volcano (unit IV). Isopach mapping of the different units, but also analyses of the distribution of material accumulated above and between prominent horizons identified at a

regional (V and S) or at a local scale ( $H_1$ ,  $H_2$ , and  $H_3$ ), indicated major changes in depositional systems in the submarine environment during the time intervals defined by these horizons. This allowed for a detailed reconstruction of the evolution of La Réunion volcanic complex since the early stage of its formation.

We were able to regard the prominent regional horizons V and S, respectively, as stratigraphic markers of the onset of the submarine explosive volcanic activity of La Réunion seamount, and of the growth of the present-day Piton des Neiges. Below the horizon S, the seismostratigraphic analysis reveals the existence of a unique volcanic center during the growth and at the emergence of La Réunion that we interpreted as representing a proto-Piton des Neiges. Isopach maps below and above the horizon S did not evidence the presence of Les Alizés volcano such as previously described in the literature. To the contrary, our study demonstrated the existence of a large proto-Piton des Neiges volcano during the first building phase of the volcanic complex and a central role of the Piton des Neiges volcano during the second phase.

Recent flank-collapsing episodes affecting the subaerial part of Piton de la Fournaise volcano is also captured in the offshore sediment record. However, seismic facies observed within the apron shows a prevalence of gradual degradation/dismantling and fallout processes since the onset of La Réunion volcanism compared to catastrophic flank collapses.

#### Acknowledgments

We thank the captain M. Houmard, officers, crew, and scientific team aboard the N/O L'Atalante for their efficient work at sea. We thank the Mauritius authorities for consent to conduct part of the FOREVER cruise in their E.E.Z. The survey in Mauritius waters would not have been possible without the help of the Mauritius Oceanographic Institute and the French Embassy. We thank the Editor, Associate Editor, and the reviewers Jean-François Lénat, and Claudia Romagnoli for their comments, which helped to improve the quality of the manuscript. We also thank Georges Boudon and Melanie Froude for additional comments on the manuscript, and Philippe Charvis for reviewing an earlier version of the manuscript. SMT (Kingdom Suite software) provided free academic licenses at IPGP and University of Pau. Most of the figures were prepared using the SMT Kingdom Suite software and the GMT software developed by P. Wessel and W. Smith. Data from the FOREVER cruise can be obtained through the French national oceanographic data center ([http://www.ifremer.fr/sismer/index\\_UK.htm](http://www.ifremer.fr/sismer/index_UK.htm)). This work was supported by CNRS-INSU. IPGP contribution 3918.

#### References

- Bachèlery, P., & Mairine, P. (1990). Evolution volcano-structurale du Piton de la Fournaise depuis 0.53 Ma. In J.-F. Lénat (Ed.), *Le volcanisme de la Réunion, Monographie*, (pp. 213–242). Clermont-Ferrand, France: Cent. Rech. Volcanol.
- Berthod, C., Michon, L., Famin, V., Bascou, J., & Bachèlery, P. (2016). Magma chamber history related to the shield building stage of Piton des Neiges volcano, La Réunion Island, EGU 2016, Vienna, 17–22 April 2016, Geophysical Research, Abstracts EGU2016-12100.
- Bonneville, A., Barriot, J.-P., & Bayer, R. (1988). Evidence From geoid data of a hot spot origin from the southern Mascarene Plateau and Mascarene Islands (Indian Ocean). *Journal of Geophysical Research*, *93*(B5), 4199–4212. <https://doi.org/10.1029/JB093iB05p04199>
- Brunet, M., Le Friant, A., Boudon, G., Lafuerza, S., Talling, P., Hornbach, M., ... IODP Expedition 340 science party (2015). Composition, geometry and emplacement dynamics of a large volcanic island landslide offshore Martinique: From volcano flank-collapse to seafloor sediment failure? *Geochemistry, Geophysics, Geosystems*, *17*, 699–724. <https://doi.org/10.1002/2015GC006034>
- Carey, S., Maria, T., & Cornell, W. (1998). Processes of volcanoclastic sedimentation during the early growth stages of Gran Canaria based on sediments from Site 953. In P. P. E. Weaver, et al. (Eds.), *Proceedings of the Ocean Drilling Program, Scientific Results* (Vol. 157, pp. 183–200). College Station, TX: Ocean Drilling Program. <https://doi.org/10.2973/odp.proc.sr.157.119.1998>
- Charvis, P., Laesanpura, A., Gallart, J., Hirn, A., Lépine, J.-C., de Voogd, B., ... Pontoise, B. (1999). Spatial distribution of hotspot material added to the lithosphere Under la Réunion, From wide-angle seismic data. *Journal of Geophysical Research*, *104*(B2), 2875–2893. <https://doi.org/10.1029/98JB02841>
- Clague, D. A., Paduan, J. B., Caress, D. W., Thomas, H., Chadwick, W. W. Jr., & Merle, S. G. (2011). Volcanic morphology of West Mata Volcano, NE Lau Basin, based on high-resolution bathymetry and depth changes. *Geochemistry, Geophysics, Geosystems*, *12*, QOAF03. <https://doi.org/10.1029/2011GC003791>
- Clague, D. A., Paduan, J. B., & Davis, A. S. (2009). Widespread Strombolian eruptions of mid-ocean ridge basalt. *Journal of Volcanology and Geothermal Research*, *180*(2–4), 171–188. <https://doi.org/10.1016/j.jvolgeores.2008.08.007>
- Cohen, J. K., & Stockwell, J. J. W. (1996). *CWP/SU: Seismic Unix release28: A free package for seismic research and processing*. Golden, CO: Center for Wave Phenomena, Colorado School of Mines.
- Deplus, C. (2006). FOREVER cruise, RV L'Atalante. <https://doi.org/10.17600/6010050>
- Deplus, C., de Voogd, B., Dyment, J., Bissessur, D., Sisavath, E., Depuiset, F., & Mercier, M. (2009). New insights on the oceanic lithosphere at La Réunion hotspot volcano, EGU 2009, Vienna, 19–24 April 2009, Geophysical Research, Abstracts 11-5728.
- Deplus, C., Le Friant, A., Boudon, G., Komorowski, J.-C., Villemant, B., Harford, C., ... Cheminée, J. L. (2001). Submarine evidence for large-scale debris avalanches in the Lesser Antilles Arc. *Earth and Planetary Science Letters*, *192*(2), 145–157. [https://doi.org/10.1016/S0012-821X\(01\)00444-7](https://doi.org/10.1016/S0012-821X(01)00444-7)
- Desvars, A., Jégo, S., Chiroleu, F., Bourhy, P., Cardinale, E., & Michault, A. (2011). Seasonality of human leptospirosis in Réunion Island (Indian Ocean) and its association with meteorological data. *PLoS One*, *6*(5), e20377. <https://doi.org/10.1371/journal.pone.0020377>
- de Voogd, B., Deplus, C., Sisavath, E., Depuiset, F., & Mercier, M. (2009). Vertical movements of the oceanic lithosphere above La Reunion hotspot, EGU 2009, Vienna, 19–24 April 2009, Geophysical Research, Abstracts 11-5754.
- de Voogd, B., Pou Palomé, S., Hirn, A., Charvis, P., Gallart, J., Rousset, D., ... Perroud, H. (1999). Vertical movements and material transport During hotspot activity: Seismic reflection profiling offshore La Réunion. *Journal of Geophysical Research*, *104*(B2), 2855–2874. <https://doi.org/10.1029/98JB02842>
- Duncan, R. A., Backman, J., & Peterson, L. (1989). Reunion hotspot activity through tertiary time: Initial results from the ocean drilling program, leg 115. *Journal of Volcanology and Geothermal Research*, *36*(1–3), 193–198. [https://doi.org/10.1016/0377-0273\(89\)90013-9](https://doi.org/10.1016/0377-0273(89)90013-9)
- Eissen, J.-P., Fouquet, Y., Hardy, D., & Ondréas, H. (2003). Recent MORB volcanoclastic explosive deposits formed between 500 and 1750 m.b.s.l. on the axis of the Mid-Atlantic Ridge, south of the Azores. In J. D. L. White, J. L. Smellie, & D. A. Clague (Eds.), *Explosive Subaqueous Volcanism* (pp. 143–166). Washington, DC: American Geophysical Union. <https://doi.org/10.1029/140GM09>
- Funck, T., Dickmann, T., Rihm, R., Krastel, S., Lykke-Andersen, H., & Schmincke, H.-U. (1996). Reflection seismic investigations in the volcanoclastic apron of Gran Canaria and implications for its volcanic evolution. *Geophysical Journal International*, *125*(2), 519–536. <https://doi.org/10.1111/j.1365-246X.1996.tb00015.x>
- Funck, T., & Lykke-Andersen, H. (1998). Comparison of seismic reflection data to a synthetic seismogram in a volcanic apron at Site 953. In P. P. E. Weaver, et al. (Eds.), *Proceedings of the ODP, Science Results* (Vol. 157, pp. 3–9). College Station, TX: Ocean Drilling Program. <https://doi.org/10.2973/odp.proc.sr.157.100.1998>
- Gailler, L.-S., & Lénat, J.-F. (2010). Three-dimensional structure of the submarine flanks of La Réunion inferred from geophysical data. *Journal of Geophysical Research*, *115*, B12105. <https://doi.org/10.1029/2009JB007193>

- Gailler, L.-S., & Lénat, J.-F. (2012). Internal architecture of La Réunion (Indian Ocean) inferred from geophysical data. *Journal of Volcanology and Geothermal Research*, 221–222, 83–98. <https://doi.org/10.1016/j.jvolgeores.2012.01.015>
- Gallart, J., Driad, L., Charvis, P., Sapin, M., Hirn, A., Diaz, J., ... Sachpazi, M. (1999). Perturbation to the lithosphere along the hotspot track of La Réunion from an offshore-onshore seismic transect. *Journal of Geophysical Research*, 104(B2), 2895–2908. <https://doi.org/10.1029/98JB02840>
- Germa, A., Quidelleur, X., Labanieh, S., Chauvel, C., & Lahitte, P. (2011). The volcanic evolution of Martinique Island: Insight from K-Ar dating into the Lesser Antilles arc migration since the Oligocene. *Journal of Volcanology and Geothermal Research*, 208(3–4), 122–135.
- Gillot, P.-Y., Lefèvre, J.-C., & Nativel, P.-E. (1994). Model for the structural evolution of the volcanoes of Réunion Island. *Earth and Planetary Science Letters*, 122(3–4), 291–302. [https://doi.org/10.1016/0012-821X\(94\)90003-5](https://doi.org/10.1016/0012-821X(94)90003-5)
- Gillot, P.-Y., & Nativel, P. (1989). Eruptive history of the Piton de la Fournaise volcano, Reunion Island, Indian Ocean. *Journal of Volcanology and Geothermal Research*, 36(1–3), 53–65. [https://doi.org/10.1016/0377-0273\(89\)90005-X](https://doi.org/10.1016/0377-0273(89)90005-X)
- Krastel, S., & Schmincke, H.-U. (2002). Crustal structure of northern Gran Canaria, Canary Islands, deduced from active seismic tomography. *Journal of Volcanology and Geothermal Research*, 115(1–2), 153–177. [https://doi.org/10.1016/S0377-0273\(01\)00313-4](https://doi.org/10.1016/S0377-0273(01)00313-4)
- Labazuy, P. (1996). Recurrent landslides events on the submarine flank of Piton de la Fournaise volcano (Reunion Island). *Geological Society, London, Special Publications*, 110(1), 295–306. <https://doi.org/10.1144/GSL.SP.1996.110.01.23>
- Le Friant, A., Boudon, G., Deplus, C., & Villemant, B. (2003). Large scale flank collapse events during the activity of Montagne Pelée, Martinique, Lesser Antilles. *Journal of Geophysical Research*, 108(B1), 2055. <https://doi.org/10.1029/2001JB001624>
- Le Friant, A., Ishizuka, O., Boudon, G., Palmer, M. R., Talling, P. J., Villemant, B., ... Watt, S. F. L. (2015). Submarine record of volcanic island construction and collapse in the Lesser Antilles arc: First scientific drilling of submarine volcanic island landslides by IODP Expedition 340. *Geochemistry, Geophysics, Geosystems*, 16, 420–442. <https://doi.org/10.1002/2014GC005652>
- Le Friant, A., Lebas, E., Clément, V., Boudon, G., Deplus, C., de Voogd, B., & Bachèlery, P. (2011). A new model for the evolution of La Réunion volcanic complex from complete marine geophysical surveys. *Geophysical Research Letters*, 38, L09312. <https://doi.org/10.1029/2011GL047489>
- Lénat, J.-F., Gibert-Malengreau, B., & Galdéano, A. (2001). A new model for the evolution of the volcanic island of Réunion (Indian Ocean). *Journal of Geophysical Research*, 106(B5), 8645–8663. <https://doi.org/10.1029/2000JB900448>
- Lénat, J.-F., Vincent, P., & Bachèlery, P. (1989). The offshore continuation of an active basaltic volcano: Piton de la Fournaise (Réunion Island, Indian Ocean); structural and geomorphological interpretation from sea beam mapping. *Journal of Volcanology and Geothermal Research*, 36(1–3), 1–36. [https://doi.org/10.1016/0377-0273\(89\)90003-6](https://doi.org/10.1016/0377-0273(89)90003-6)
- Leslie, S. C., Moore, G. F., Morgan, J. K., & Hills, D. J. (2002). Seismic stratigraphy of the Frontal Hawaiian Moat: Implications for sedimentary processes at the leading edge of an oceanic hotspot trace. *Marine Geology*, 184(1–2), 143–162. [https://doi.org/10.1016/S0025-3227\(01\)00284-5](https://doi.org/10.1016/S0025-3227(01)00284-5)
- Malengreau, B., Lénat, J.-F., & Froger, J.-L. (1999). Structure of Réunion Island (Indian Ocean) inferred from the interpretation of gravity anomalies. *Journal of Volcanology and Geothermal Research*, 88(3), 131–146. [https://doi.org/10.1016/S0377-0273\(98\)00114-0](https://doi.org/10.1016/S0377-0273(98)00114-0)
- Masson, D., Watts, A., Gee, M. J., Urgeles, R., Mitchell, N., Le Bas, T., & Canals, M. (2002). Slope failures on the flanks of the western Canary Islands. *Earth-Science Reviews*, 57(1–2), 1–35. [https://doi.org/10.1016/S0012-8252\(01\)00069-1](https://doi.org/10.1016/S0012-8252(01)00069-1)
- Mazuel, A., Sisavath, E., Babonneau, N., Jorry, S. J., Bachèlery, P., & Delacourt, C. (2016). Turbidity current activity along the flanks of a volcanic edifice: The mafate volcanoclastic complex, La Réunion Island, Indian Ocean. *Sedimentary Geology*, 335, 34–50. <https://doi.org/10.1016/j.sedgeo.2016.01.020>
- McDougall, I. (1971). The geochronology and evolution of the young volcanic island of Réunion, Indian Ocean. *Geochimica et Cosmochimica Acta*, 35(3), 261–288. [https://doi.org/10.1016/0016-7037\(71\)90037-8](https://doi.org/10.1016/0016-7037(71)90037-8)
- McGuire, W. J. (1996). Volcano instability: A review of contemporary themes. *Geological Society, London, Special Publications*, 110(1), 1–23. <https://doi.org/10.1144/GSL.SP.1996.110.01.01>
- Menard, H. W. (1956). Archipelagic aprons. *American Association of Petroleum Geologists Bulletin*, 40, 2195–2210.
- Merle, O., Mairine, P., Michon, L., Bachèlery, P., & Smietana, M. (2010). Calderas, landslides and paleo-canyons on Piton de la Fournaise volcano (La Réunion Island, Indian Ocean). *Journal of Volcanology and Geothermal Research*, 189(1–2), 131–142. <https://doi.org/10.1016/j.jvolgeores.2009.11.001>
- Mitchell, N. C., Dade, W. B., & Masson, D. G. (2003). Erosion of the submarine flanks of the Canary Islands. *Journal of Geophysical Research*, 108(F1), 6002. <https://doi.org/10.1029/2002JF000003>
- Moore, J. G., Clague, D. A., Holcomb, R. T., Lipman, P. W., Normark, W. R., & Torresan, M. E. (1989). Prodigious submarine landslides on the Hawaiian ridge. *Journal of Geophysical Research*, 94(B12), 17,465–17,484. <https://doi.org/10.1029/JB094iB12p17465>
- Moore, J. G., Normark, W. R., & Holcomb, R. T. (1994). Giant Hawaiian landslides. *Annual Review of Earth and Planetary Sciences*, 22(1), 119–144. <https://doi.org/10.1146/annurev.ea.22.050194.001003>
- Oehler, J.-F., Labazuy, P., & Lénat, J.-F. (2004). Recurrence of major flank landslides during the last 2-Ma-history of Reunion Island. *Bulletin of Volcanology*, 66(7), 585–598. <https://doi.org/10.1007/s00445-004-0341-2>
- Oehler, J.-F., Lénat, J.-F., & Labazuy, P. (2008). Growth and collapse of the Réunion Island volcanoes. *Bulletin of Volcanology*, 70(6), 717–742. <https://doi.org/10.1007/s00445-007-0163-0>
- Posamentier, H. W., & Kolla, V. (2003). Seismic geomorphology and stratigraphy of depositional elements in deep-water settings. *Journal of Sedimentary Research*, 73(3), 367–388. <https://doi.org/10.1306/111302730367>
- Pou Palomé, S. (1997). Structure et évolution de l'édifice volcanique de point chaud de la Réunion: Traitement et interprétation des profils de sismique réflexion de la campagne REUSIS (PhD thesis). Pau, France: Université de Pau.
- Quidelleur, X., Holt, J. W., Salvany, T., & Bouquerel, H. (2010). New K-Ar ages from La Montagne massif, Réunion Island (Indian Ocean), supporting two geomagnetic events in the time period 2.2–2.0 Ma. *Geophysical Journal International*, 182, 699–710. <https://doi.org/10.1111/j.1365-246X.2010.04651.x>
- Rançon, J. P., Lerebour, P., & Augé, T. (1989). The Grand Brule exploration drilling: New data on the deep framework of the Piton de la Fournaise volcano. Part 1: Lithostratigraphic units and volcanostructural implications. *Journal of Volcanology and Geothermal Research*, 36(1–3), 113–127. [https://doi.org/10.1016/0377-0273\(89\)90008-5](https://doi.org/10.1016/0377-0273(89)90008-5)
- Rees, B. A., Detrick, R. S., & Coakley, B. J. (1993). Seismic stratigraphy of the Hawaiian flexural moat. *Geological Society of America Bulletin*, 105(2), 189–205. [https://doi.org/10.1130/0016-7606\(1993\)105%3C0189:SSOTHF%3E2.3.CO;2](https://doi.org/10.1130/0016-7606(1993)105%3C0189:SSOTHF%3E2.3.CO;2)
- Rivals, P. (1950). Histoire géologique de l'île de La Réunion (PhD thesis). Toulouse, France: Université de Toulouse.
- Romagnoli, C., Casalbore, D., Bosman, A., Braga, R., & Chiocci, F. L. (2013). Submarine structure of Vulcano volcano (Aeolian Islands) revealed by high-resolution bathymetry and seismo-acoustic data. *Marine Geology*, 338, 30–45. <https://doi.org/10.1016/j.margeo.2012.12.002>
- Romagnoli, C., & Jakobsson, S. P. (2015). Post-eruptive morphological evolution of island volcanoes: Surtsey as a modern case study. *Geomorphology*, 250, 384–396. <https://doi.org/10.1016/j.geomorph.2015.09.016>



- Rousset, D., Bonneville, A., & Lénat, J.-F. (1987). Detailed gravity study of the offshore structure of Piton de la Fournaise volcano, Réunion Island. *Bulletin of Volcanology*, 49(6), 713–722. <https://doi.org/10.1007/BF01079822>
- Saint-Ange, F., Savoye, B., Michon, L., Bachèlery, P., Deplus, C., de Voogd, B., ... Boudon, G. (2011). A volcanoclastic deep-sea fan off La Réunion Island (Indian Ocean): Gradualism versus catastrophism. *Geology*, 39(3), 271–274. <https://doi.org/10.1130/G31478.1>
- Salvany, T., Lahitte, P., Nativel, P., & Gillot, P.-Y. (2012). Geomorphic evolution of the piton des Neiges volcano (Réunion Island, Indian Ocean): Competition between volcanic construction and erosion since 1.4Ma. *Geomorphology*, 136(1), 132–147. <https://doi.org/10.1016/j.geomorph.2011.06.009>
- Schmincke, H.-U., & Sumita, M. (1998). Volcanic evolution of Gran Canaria reconstructed from apron sediments: Synthesis of VICAP project drilling. In P. P. E. Weaver, et al. (Eds.), *Proceedings of the Ocean Drilling Program, Scientific Results* (Vol. 157, pp. 443–469). College Station, TX: Ocean Drilling Program. <https://doi.org/10.2973/odp.proc.sr.157.135.1998>
- Schnur, S. R., Chadwick, W. W. Jr., Embley, R. W., Ferrini, V. L., de Ronde, C. E. J., Cashman, K. V., ... Matsumoto, H. (2017). A decade of volcanic construction and destruction at the summit of NW Rota-1 seamount: 2004–2014. *Journal of Geophysical Research: Solid Earth*, 122, 1558–1584. <https://doi.org/10.1002/2016JB013742>
- Sisavath, E., Babonneau, N., Saint-Ange, F., Bachèlery, P., Jorry, S. J., Deplus, C., ... Savoye, B. (2011). Morphology and sedimentary architecture of a modern volcanoclastic turbidite system: The Cilaos fan, offshore La Réunion Island. *Marine Geology*, 288(1-4), 1–17. <https://doi.org/10.1016/j.margeo.2011.06.011>
- Smietana, M. (2011). Pétrologie, géochronologie (K-Ar) et géochimie élémentaire et isotopique (Sr, Nd, Hf, Pb) de laves anciennes de La Réunion: Implications sur la construction de l'édifice volcanique (PhD thesis). Université de La Réunion.
- Smith, W. H. F., & Sandwell, D. T. (1997). Global seafloor topography from satellite altimetry and ship depth soundings. *Science*, 277, 1957–1962.
- Sohn, R. A., Willis, C., Humphris, S., Shank, T. M., Singh, H., Edmonds, H. N., ... Soule, A. (2008). Explosive volcanism on the ultraslow-spreading Gakkel ridge, Arctic Ocean. *Nature*, 453(7199), 1236–1238. <https://doi.org/10.1038/nature07075>
- Staudigel, H., & Clague, D. A. (2010). The geological history of deep-sea volcanoes. *Oceanography*, 23(01), 58–71. <https://doi.org/10.5670/oceanog.2010.62>
- Stearns, H. T. (1946). Geology of the Hawaiian Islands: Hawaii (Terr.), division of hydrography. *Bulletin*, 8, 106.
- Upton, B. G. J., & Wadsworth, W. J. (1965). Geology of Réunion Island, Indian Ocean. *Nature*, 207, 151–154.
- Upton, B. G. J., & Wadsworth, W. J. (1969). Early volcanic rocks of Réunion and their tectonic significance. *Bulletin of Volcanology*, 33(4), 1246–1268. <https://doi.org/10.1007/BF02597720>
- Urgeles, R., Canals, M., Baraza, J., & Alonso, B. (1998). Seismostratigraphy of the western flanks of El Hierro and La Palma (Canary Islands): A record of Canary Islands volcanism. *Marine Geology*, 146(1-4), 225–241. [https://doi.org/10.1016/S0025-3227\(97\)00130-8](https://doi.org/10.1016/S0025-3227(97)00130-8)
- Urgeles, R., Canals, M., Baraza, J., Alonso, B., & Masson, D. (1997). The most recent megalandslides of the Canary Islands: El Golfo debris avalanche and Canary debris flow, west El Hierro Island. *Journal of Geophysical Research*, 102(B9), 20,305–20,323. <https://doi.org/10.1029/97JB00649>
- Walker, S. L., Baker, E. T., Resing, J. A., Chadwick, W. W. Jr., Lebon, G. T., Lupton, J. E., & Merle, S. G. (2008). Eruption-fed particle plumes and volcanoclastic deposits at a submarine volcano: NW Rota-1, Mariana Arc. *Journal of Geophysical Research*, 113, B08S11. <https://doi.org/10.1029/2007JB005441>
- Washington, H. S. (1909). The submarine eruption of 1831 and 1891 near Pantelleria. *American Journal of Science*, 27, 131–150.
- Wessel, P., & Smith, W. H. F. (2004). The Generic Mapping Tools (GMT) version 4 technical reference & cookbook, SOEST/NOAA.
- Wolfe, C. J., McNutt, M. K., & Detrick, R. S. (1994). The Marquesas archipelagic apron: Seismic stratigraphy and implications for volcano growth, mass wasting, and crustal underplating. *Journal of Geophysical Research*, 99(B7), 13,591–13,608. <https://doi.org/10.1029/94JB00686>